FEMS Microbiology Reviews, 2023, 47, 1–21
DOI: 10.1093/femsre/fuad052
Advance access publication date: 15 September 2023
Review Article

Type II bacterial toxin–antitoxins: hypotheses, facts, and the newfound plethora of the PezAT system

Wai Ting Chan[1], Maria Pilar Garcillán-Barcia[2], Chew Chieng Yeo[3,*], Manuel Espinosa[1,*]

[1]Centro de Investigaciones Biológicas Margarita Salas, Consejo Superior de Investigaciones Científicas, Ramiro de Maeztu, 9, 28040 Madrid, Spain
[2]Instituto de Biomedicina y Biotecnología de Cantabria (IBBTEC), Universidad de Cantabria-Consejo Superior de Investigaciones Científicas, C/Albert Einstein 22, PCTCAN, 39011 Santander, Spain
[3]Centre for Research in Infectious Diseases and Biotechnology (CeRIDB), Faculty of Medicine, Universiti Sultan Zainal Abidin, Jalan Sultan Mahumd, 20400 Kuala Terengganu, Malaysia
*Corresponding author. Chew Chieng Yeo, Centre for Research in Infectious Diseases and Biotechnology (CeRIDB), Faculty of Medicine, Universiti Sultan Zainal Abidin, Jalan Sultan Mahumd, 20400 Kuala Terengganu, Malaysia. E-mail: chewchieng@gmail.com; Manuel Espinosa, Centro de Investigaciones Biológicas Margarita Salas, Consejo Superior de Investigaciones Científicas, Ramiro de Maeztu, 9, 28040 Madrid, Spain. E-mail: mespinosa@cib.csic.es
Dedicated to the late Professor Laura Frost, a dear colleague and a dear friend
Editor: [Grzegorz Wegrzyn]

Abstract

Toxin–antitoxin (TA) systems are entities found in the prokaryotic genomes, with eight reported types. Type II, the best characterized, is comprised of two genes organized as an operon. Whereas toxins impair growth, the cognate antitoxin neutralizes its activity. TAs appeared to be involved in plasmid maintenance, persistence, virulence, and defence against bacteriophages. Most Type II toxins target the bacterial translational machinery. They seem to be antecessors of Higher Eukaryotes and Prokaryotes Nucleotide-binding (HEPN) RNases, minimal nucleotidyltransferase domains, or CRISPR–Cas systems. A total of four TAs encoded by *Streptococcus pneumoniae*, RelBE, YefMYoeB, Phd-Doc, and HicAB, belong to HEPN-RNases. The fifth is represented by PezAT/Epsilon–Zeta. PezT/Zeta toxins phosphorylate the peptidoglycan precursors, thereby blocking cell wall synthesis. We explore the body of knowledge (facts) and hypotheses procured for Type II TAs and analyse the data accumulated on the PezAT family. Bioinformatics analyses showed that homologues of PezT/Zeta toxin are abundantly distributed among 14 bacterial phyla mostly in Proteobacteria (48%), Firmicutes (27%), and Actinobacteria (18%), showing the widespread distribution of this TA. The *pezAT* locus was found to be mainly chromosomally encoded whereas its homologue, the tripartite *omega–epsilon–zeta* locus, was found mostly on plasmids. We found several orphan *pezT/zeta* toxins, unaccompanied by a cognate antitoxin.

Keywords: bacterial type II toxin–antitoxins, cell wall biosynthesis, pathogenicity islands, pneumococcus

Abbreviations

asRNA:	antisense RNA
G:	Gram
HTH:	helix-turn-helix
IS:	insertion sequence
MGEs:	mobile genetic elements
nt:	nucleotide(s)
PPI:	protein–protein interaction
RHH:	ribbon-helix-helix
TA(s):	toxin–antitoxin(s)
UNAG:	uridine-diphosphate-*N*-acetylglucosamine
UNAG-3P:	uridine-*N*-acetylglucosamine-3´-phosphate
wt :	*wild type*

Introduction

Before the COVID-19 pandemic, bacterial infections were the second highest cause of human mortality after coronary heart disease, according to the Global Burden of Diseases, Injuries, and Risk Factors Study from 2019 (Ikuta et al. 2022). With an estimated 7.7 million deaths per year as well as many millions more hospitalized, these infections constitute a huge toll on human lives and a heavy economic burden to society. These resilient and increasing infections are, at least partly, due to the enormous selective pressure that has been laid on bacteria over the years by the overuse and abuse of antibiotics in clinical and veterinary treatments primarily for (i) treatment of bacterial infections, (ii) prophylaxis, and/or (iii) dietary supplement in farming (Murray et al. 2022, Mulchandani et al. 2023). Pathogenic and commensal bacteria have equally suffered similar pressure. Such stress upon the bacterial world has led to the selection of species that exhibit high levels of resistance to multiple antibiotics ('superbugs'). Many of the superbugs are pathogenic or opportunistic, whereas other innocuous bacteria may act as a reservoir of DNA, i.e. shared among all the bacterial population by processes of vertical and horizontal gene transfer (HGT; Bravo et al. 2018). Throughout the years of confronting antibiotic-resistant bacteria, the idea that we must 'fight' against them and that it will be a 'battle that we cannot lose' has taken firm ground (Bravo et al. 2018, Garcillán-Barcia et al. 2022). The need to grasp the dynamics of the appearance of multiple antibiotic resistances and their relationship with gene transfer processes is linked to other worldwide evolutionary im-

Received 26 June 2023; **revised** 24 August 2023; **accepted** 7 September 2023

pacts of anthropogenic activities on the entire biosphere (Michael et al. 2021).

The abovementioned belligerent concepts have been re-examined in light of the *One Earth* concept developed by us (Bravo et al. 2018, Garcillán-Barcia et al. 2022). Understandably, the need to find novel strategies and targets to cope with diseases caused by superbugs is urgent. We must take care of human survival in a world where infections by superbugs are increasing steadily: the World Health Organisation has predicted a human toll of ∼10 million superbugs-related deaths per year by 2050 (https://www.who.int/news-room/fact-sheets/detail/antimicrobial-resistance). Several solutions have been outlined (Chan et al. 2015, Bravo et al. 2018, Nadeem et al. 2020, Hobson et al. 2021), and most of them involve the identification of novel targets and the development of novel strategies. Some of the approaches suggested include (i) bacteriophage (phage) therapy, (ii) inhibitors of protein–protein interactions (PPIs), (iii) interference with the bacterial mobile genetic elements (MGEs) to inhibit HGT processes, (iv) targeting virulence traits, (v) inhibition of secretion systems, (vi) antisense RNAs, and (vii) search and/or design of small molecules, termed fragments (< 300 Da), with low affinities that can be optimized into drug lead compounds (Chan et al. 2015, Bravo et al. 2018, Kim et al. 2022, Shi et al. 2023). A very different path just beginning to be explored is the possibility of developing compounds that do not kill bacteria, but instead act by targeting virulence factors such as bacterial toxins or the proteins controlling microbial quorum sensing, or biofilm formation. Moreover, an interesting approach contemplates the use of bacterial-encoded toxin–antitoxins (TAs) as possible antibacterials (Chan et al. 2015, Równicki et al. 2020, Kim et al. 2022), which will be briefly reviewed below (see: *Type II TAs as possible targets for antibacterials*).

Bacterial TA operons

Within their natural habitats, bacteria strive and expand by employing regulatory networks, the *nichome* (Bravo et al. 2018), which contribute to their successful colonization of new niches in fluctuating environments. Under these variable conditions, bacteria are frequently confronted with stressful situations where they must cope for their survival. Among the genes involved in the bacterial responses, the TA systems comprise a compelling group of genes that regulate the response of microorganisms to the many stresses related to their lifestyle. TAs are present in the chromosomes of the majority of bacterial species and their MGEs. They are currently grouped into eight different types (designated types I–VIII) depending upon the composition of the toxin and its mode of action (Lehnherr et al. 1993, Gerdes et al. 2005, Gerdes and Maisonneuve 2012, Díaz-Orejas et al. 2017, Harms et al. 2018, Song and Wood 2020a, Qiu et al. 2022). Within the same TA type, different protein families are included and in this sense, it will be used in this review. TAs are generally composed of two genes organized as a single operon, with the antitoxin gene usually (but not always) preceding the toxin-encoding gene. Whereas the stable toxin impairs bacterial growth, the unstable antitoxin neutralizes the toxin effect by binding to it and occluding the potentially dangerous amino acid residues. Toxins are always proteins, except for the recently added type VIII family, which is composed of two RNAs (Qiu et al. 2022), whereas the antitoxin (the less conserved of the pair) could be a protein or a small RNA. More than one member of each TA type may be present in the same host, either in the chromosome (Lobato-Márquez et al. 2016, Page and Peti 2016, Akarsu et al. 2019, Jurėnas et al. 2022, Qiu et al. 2022) or in MGEs (Harms et al. 2018). Two major TAs databases, TADB 2.0 (Xie et al. 2018), and TASmania (Akarsu et al., 2019) are available at https://bioinfo-mml.sjtu.edu.cn/TADB2/index.php and https://shiny.bioinformatics.unibe.ch/apps/tasmania/, respectively.

Several roles have been ascribed to TAs, some of which have been revisited recently (Song and Wood 2020a, Jurėnas et al. 2022, Bonabal and Darfeuille 2023). Soon after their discovery, their main role was assigned to participate in the stable maintenance (Ogura and Hiraga 1983, Jaffe et al. 1985, Bravo et al. 1988). The "post-segregational killing" concept was used for the first time by Gerdes et al in 1986 (Gerdes et al., 1986). Various other roles of TAs participating in persistence, bacterial virulence, selfish DNA and, defence against phage infections, among others, have been suggested (Pecota and Wood 1996, Díaz-Orejas et al. 2017, Rosendahl et al. 2020, Jurėnas et al. 2022, LeRoux and Laub 2022, Qiu et al. 2022). However, some of their functions are still obscure and subject to debate (De Bruyn et al. 2021). An attractive proposal contemplates that the main, if not the only, role of the TAs is to participate in bacteriophage infection inhibition (Song and Wood 2020b). However, it seems a minimalistic approach, since several reports indicate that triggering TAs may lead to bacterial virulence and persistence, i.e. cells that become dormant or have a reduced growth rate and become highly tolerant to bactericidal antibiotics (Lioy et al. 2012, Wen et al. 2014a, b, Paul et al. 2019, Zhang et al. 2020, Singh et al. 2021, Sonika et al. 2023). Furthermore, transient toxin Zeta expression reduced the growth rate and inhibited phage SPP1 intracellular amplification, and the phage infective cycle resumed after the expression of antitoxin Epsilon (Moreno-del Álamo et al. 2020). We have to consider that some of the 'classical' points of view on virulence and pathogenesis can be questionable because they can be due to the over-response of the host (i.e. human) immune system and they have been wrongly attributed to virulence factors encoded by the bacteria (Margolis and Levin 2007). Further, to contemplate virulence factors as limited only to pathogens is to exclude commensal/opportunistic bacteria as always harmless, which is not the case (Wu et al. 2008). Still, we cannot rule out the participation of TAs in bacterial virulence by (i) augmenting the survival of the pathogen inside the host, (ii) inducing the synthesis of virulence factors, and (iii) participating in biofilm formation (Chan et al. 2018, Mahmoudi et al. 2022, Lewis et al. 2023). Thus, the functional relationships of TAs with bacterial adaptation to novel environmental niches cannot be discarded (Kamruzzaman et al. 2021). Further, the role of TAs in the survival of bacteria in environments subjected to changes seems to be well established (Kędzierska and Hayes 2016a, Harms et al. 2018, Fraikin et al. 2020, Jurėnas and Van Melderen 2020, Jurėnas et al. 2022).

Type II TAs

So far, the best-characterized family is that of the Type II TAs, and we shall refer only to them in this review. These TAs are generally organized as two proteins encoded in a single transcriptional unit: one labile antitoxin that usually precedes the stable toxin (Fig. 1). Type II TAs are found in most bacteria, archaea, and MGEs (Leplae et al. 2011, Chan et al. 2016, Jurėnas et al. 2022, Qiu et al. 2022). Maintenance of genetic information, which is selfish behaviour, would appear to be the major role of Type II TAs associated with MGEs. However, chromosomal TAs may contribute largely to functions associated with the bacterial lifestyle, including the supervision and management of different stresses, virulence, and pathogenesis. Under steady-state growth conditions, antitoxin and toxin proteins generate a stable complex that binds to its promoter and represses the syn-

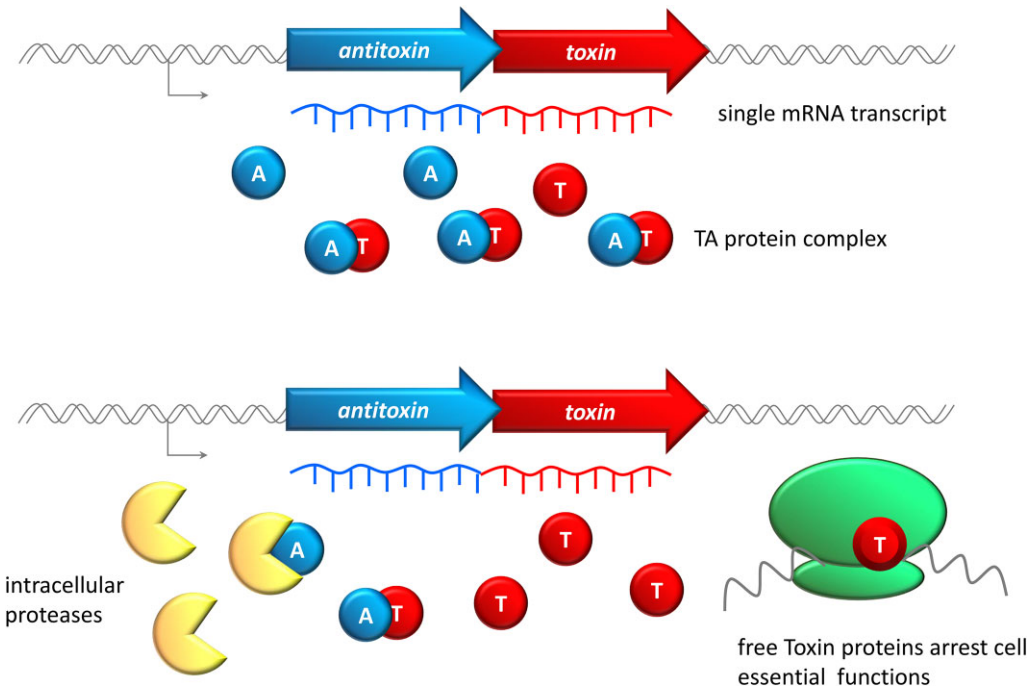

Figure 1. Common genetic organization of Type II bacterial TAs. The two participating genes encode the antitoxin (blue) that precedes the toxin gene (red). Both are transcribed from a single promoter (grey arrow with the arrowhead pointing to the direction of transcription) as a single mRNA molecule. The two proteins generate a stable complex. Under stressful conditions, intracellular proteases (yellow) cleave and inactivate the antitoxin molecules, releasing the cognate toxin that would arrest essential cell functions.

thesis of the TA mRNA. In this complex, a tetramer of the antitoxin usually sandwiches a dimer of the toxin forming a tight non-toxic hetero–hexameric complex because the toxic amino acid residues are hidden by the antitoxin residues (Arbing et al. 2010). Configurations other than heterohexamers have been detected for TA proteins, as in the case of the recently solved structures of the complex between antitoxin VPA0769 and toxin VPA0770 from *Vibrio parahaemolyticus* in which W-shaped heterohexamers and doughnut-shaped heterododecamers were observed depending upon protein concentration (Zhang et al. 2023). In the above cases, the antitoxin wraps the toxin and occludes the amino acid residues of the active site of the toxin, and thus the lethal effect of the toxin is counteracted (Sterckx et al. 2012, 2016, Xue et al. 2020, Moreno-Córdoba et al. 2021, Zhang et al. 2023). Under stressful conditions (like temperature increases, lack of nutrients, presence of antibiotics, and so on), the antitoxins are selectively cleaved by intracellular ATPases associated with diverse cellular activities (AAA^+) proteases (Lon, ClpX), probably because the antitoxins appear to be partially unfolded and, consequently, more prone to degradation (Van Melderen et al. 1996, Loris et al. 2003, Cherny et al. 2005, Loris and Garcia-Pino 2014, Chan et al. 2016, Kędzierska and Hayes 2016b, Page and Peti 2016). The proteolytic attack would lead to the release of the toxin in a free form and the arrest of cell growth, dormancy (Brzozowska and Zielenkiewicz 2013, 2014), or even cell death, as in the cases of postsegregational killing subsequent to the loss of plasmid-bearing TAs (Bertram and Schuster 2014, Hernández-Arriaga et al. 2014). These points of view have been recently questioned on the basis that TAs participate in processes leading to (i) stress-derived reduction of the cell metabolism, (ii) inhibition of phage infection, and (iii) biofilm formation (Song and Wood 2018, 2020a, b). Further, under physiological conditions (steady-state) evidence that toxins cause cell death or persistence seems to be scarce (Song and Wood 2020b); as reviewed by Bordes and Genevaux (2021). In the case of the TAs encoded by the pathogenic Gram-positive (G+) bacterium *Streptococcus pneumoniae*, we showed that, under physiological conditions, two TAs (*relBE* and *yefM-yoeB*) cooperatively participated in biofilm formation (Chan et al. 2018). Similar information has been reported for the Gram-negative (G−) bacterium, *Pseudomonas aeruginosa* (Mahmoudi et al. 2022), and in the archaeal thermoacidophile *Sulfolobus acidocaldarius* (Lewis et al. 2023). Interestingly, deletion of the *pezAT* operon did not influence biofilm formation (Chan and Espinosa 2016a). Whether these differences are due to the mechanism of action of the former (proteins interfering with the translation machinery) compared to the latter (cell-wall disruption) is not known at present.

Transcriptional regulation of each TA operon may differ among the different Type II families, but in general, it appears that the antitoxins have a weak binding affinity for their DNA target, which is usually located within or upstream of the promoter region of the operon (Kędzierska and Hayes 2016a). The formation of the TA protein complex seems to increase the affinity of the antitoxin for its DNA target (Loris and Garcia-Pino 2014, Chan et al. 2016, De Bruyn et al. 2021) with the exception of MqsRA (Brown et al. 2013). Interestingly, even among members of the same family of antitoxins, different DNA-binding domains and mechanisms for transcriptional control have been observed (De Bruyn et al. 2021). This could be due to the lack of conservation among the antitoxin proteins, whereas their toxin counterparts are much more conserved (Zhang et al. 2020). More complex situations in the regulation of Type II TA expression have derived from the recent finding of a novel tripartite locus, composed of a RelE2 toxin, a RelB2 antitoxin, and antisense (as)RNA encoded by *Mycobacterium tuberculosis* (Dawson et al. 2022). This new member, termed Type IIb, is characterized thus because it is the combination of the antitoxin and the antisense RNA that regulates the expression of the toxin

gene instead of just the antitoxin alone as in most Type II TAs. And yet, there is the proposal of adding another subtype of the Type II TAs, as it has been reported that the *P. aeruginosa* PacTA pair exhibits a new activity and participates in the regulation of iron homeostasis, a crucial pathway that modulates the bacteria lifestyle (Song et al. 2022, Li et al. 2023).

Targets of Type II TAs

The biochemical activities of the toxins are different but in most cases, they mark important cell functions at the levels of chromosome structure, translation, or integrity of the cell wall. Most Type II toxins target the cellular translation machinery (Yamaguchi and Inouye 2011, 2013, Harms et al. 2018). However, they act at different levels such as (i) the cleavage of free mRNA in a sequence-specific manner, like MazF (Zhang et al. 2003), (ii) degradation of the mRNA associated with ribosomes, like RelE (Pedersen et al. 2003), (iii) the cleavage of the initiator tRNA, like VapC (Winther et al. 2013), (iv) the transfer of adenosine 5´monophosphate (AMPylation) to the EF-Tu elongation factor by toxins like HipA or Doc (Schumacher et al., 2009). These results have been questioned by more recent investigations that showed that the AMPylation activity could be due to an in vitro artefact because HipA phosphorylates the host Glutamyl-tRNA-synthetase both in vitro and in vivo and thereby inhibits translation (Kaspy et al., 2013); (Germain et al., 2013). These results were later confirmed (Semanjski et al., 2018); (Vang Nielsen et al., 2019) or Doc (Schumacher et al. 2009, Cruz et al. 2014), or (v) more complex processes, exemplified by PacT that inhibits translation by acetylation of amino acyl-tRNAs and, at the same time, binds to the Fur regulatory protein, involved in the uptake of iron (Song et al. 2022). Less frequent seem to be those toxins that target the machinery involved in DNA replication by direct inhibition or by AMPylation of the DNA gyrase and/or the DNA topoisomerase. They are exemplified by CcdB from plasmid F, one of the earliest discovered TA toxins (Bernard and Couturier 1992), the ParE toxin encoded by the chromosome of *Vibrio cholerae* (Yuan et al. 2010), and FicT, from *Bartonella schoenbuchensis* (Harms et al. 2015, 2016). Finally, there is a class of toxins that direct their poisonous activity toward cell integrity. They are represented by the Zeta toxin from the *S. agalactiae* plasmid pSM19035 (Ceglowski et al. 1993, Lioy et al. 2012, Senior et al. 2020, Tong et al. 2021, Varadi et al. 2022) and by the chromosomally encoded PezT from *S. pneumoniae* (Khoo et al. 2007). These toxins block the synthesis of the bacterial cell wall by phosphorylation of precursors of the peptidoglycan (Mutschler et al. 2011).

Type II TAs as possible antibacterials

The need to find novel targets against superbugs, in conjunction with recent viral epidemics and pandemics, fuelled the field of drug discovery to unprecedented speed. In the case of bacterial infections, the search for novel molecules that may act as antibacterials have been reinforced by the enormous advances achieved in Artificial Intelligence (AI) through deep learning techniques (Ferruz et al. 2022, Schleif and Espinosa 2022) and a new antibiotic against *Acinetobacter baumanii* has been recently discovered by the use of AI (Liu et al. 2023). The pipeline for the discovery of novel lead compounds includes finding new products from libraries of natural or biosynthetic origins and docking assays of likely candidates on known structures of desired targets (Meyers et al. 2021). The development of the AlphaFold2 program, devoted to the prediction of protein structures with very high accuracy has facilitated the search for candidates of compounds that could interact with proteins of unknown (but predictable) three-dimensional structures (Senior et al. 2020, Tong et al. 2021, Varadi et al. 2022). Alternatively, novel techniques, termed 'skeletal editing', that permit the deletion, addition, or switch of atoms within a single molecule have revolutionized the approaches to drug discovery (Peplow 2023).

One potential candidate to develop novel antibacterials would include the bacterial toxin counterparts of the TA systems candidates, especially because they seem not to be present in eukaryotic cells, an important consideration for their development as novel drugs (Chan et al. 2015, 2016, Kim et al. 2022, Bonabal and Darfeuille 2023). Despite being an attractive field for research of novel antibacterials, the possible druggability of TAs presents several problems to be solved before approaching this subject, namely (i) TAs are redundant, i.e. there can be several copies of the same (or similar) pair in the bacterial chromosome, making it challenging in the selection of a particular pair, (ii) each TA pair would need a target validation, (iii) the off-target activity (selectivity and specificity) of any TA candidate can be difficult to assess, and (iv) choosing very frequent TA pairs may substantially affect the human microbiome, which is an undesirable side-effect well known to antibiotic treatments. Further, cross-talks between different TAs may be exploited for their applications in Medicine (Boss and Kędzierska 2023). Despite these challenges, the toxins of the TA pairs offer possibilities as antibacterials, alone or in combination with classical antibiotics (Mutschler and Meinhart 2011, Park et al. 2013, Równicki et al. 2020, Kim et al. 2022).

To develop toxins as antibacterials, we proposed several approaches that are still valid (Chan et al. 2015, Chan and Espinosa 2016b), and amenable to be explored as follows (Fig. 2): First, to inhibit transcription of the TA pair, and thus autoregulation, leading to depletion of the intracellular concentration of the antitoxin and the release of the toxin (Fig. 2A). This approach should, of course, take into account the possible existence of an undetected asRNA, as recently reported for the RelBE-asRelE2 TA from *M. tuberculosis* (Dawson et al. 2022). Second, to inhibit translation of the antitoxin by the employment of an asRNA directed to the pairing to the first codons of the antitoxin without affecting translation of the toxin, which carries its initiation of translation signals (Fig. 2B). Silencing translation by specific asRNA or oligonucleotides has been successfully tested (Geller et al. 2013, Tsukuda et al. 2015), and this strategy could be the most successful one for the druggability of toxins because the delivery of the antibacterial could be relatively simple. Thirdly, artificial activation of intracellular proteases that would cleave the antitoxins and release the toxins has been proposed as an interesting approach (Williams and Hergenrother 2012), although it may be not so easy to achieve (Fig. 2C). A fourth approach, probably easier to develop, contemplates the identification of small molecules (fragments) that act as inhibitors of protein–protein interactions (i-PPIs; Fig. 2D) (Labbé et al. 2013). These inhibitors would disrupt the interactions between the toxin and the antitoxin, as has been reported for the Epsilon–Zeta TA pair (Lioy et al. 2010). These approaches would be facilitated by the available three-dimensional structures of several TA pairs (Chan et al. 2016, Lee and Lee 2016, Kang et al. 2018, Jurėnas and Van Melderen 2020, Zhang et al. 2020, 2023). The suitability of Type II TAs encoded by the pathogenic bacterium *M. abscessus* has been tested in a fragment-based drug-discovery approach (Kim et al. 2022). Fragments were used to bind to the *de novo*-determined antitoxin structure and those compounds that could produce conformational changes in the antitoxin were selected as lead compounds that prevented the formation of the TA complex (Kim et al. 2022), an interesting approach that has been patented

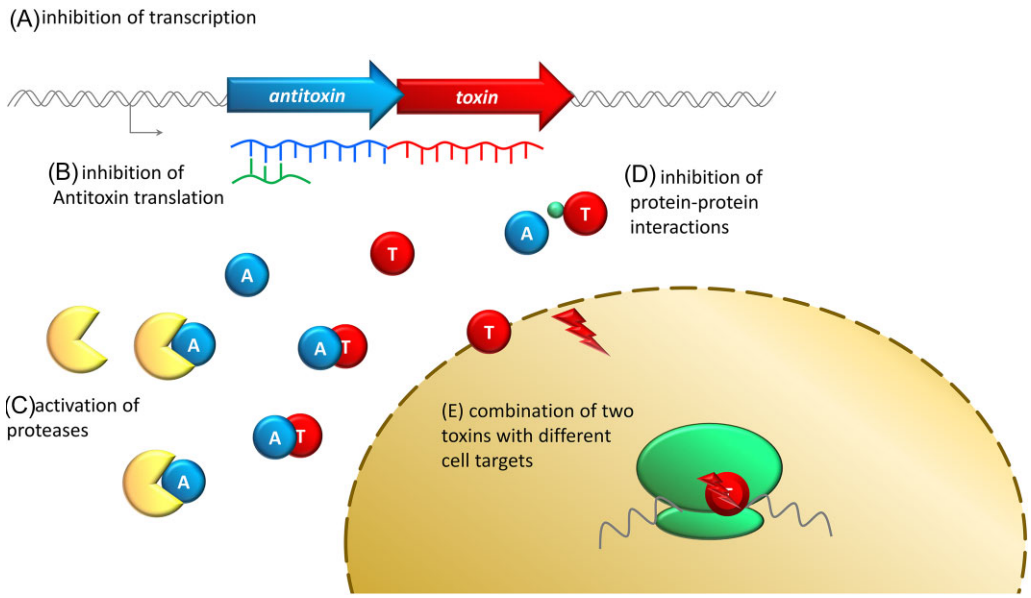

Figure 2. Possible strategies to use Type II TAs as antibacterials. These include (A) inhibition of transcription, (B) inhibition of translation by, for instance, an antisense RNA, (C) activation of intracellular proteases that would preferentially cleave the antitoxin molecules, (D) Use of molecules that act as i-PPI, thus hindering the formation of T–A complexes, and (E) combination of two toxins with different targets (cell-wall synthesis and translation machinery), thus ensuring a potentially deadly antibacterial.

(https://patents.google.com/patent/KR102097040B1/en). This approach should open pathways to develop novel antibacterials, provided that the aforementioned druggability precautions are considered. Finally, combining two toxins with different targets would be the most compelling approach. In this case, two excellent candidates would be MazF, which targets translation (Inouye 2006), and PezT, which targets cell-wall synthesis (Mutschler and Meinhart 2011). Such a combination could lead to an extremely useful broad-spectrum drug (Fig. 2E).

Type II TAs encoded by S. *pneumoniae*

Streptococcus pneumoniae (the pneumococcus) is an opportunistic G+ bacterium that colonizes the nasopharynx tract of 75% of healthy humans (Gamez and Hammerschmidt 2012). Under hospital conditions or in immunocompromised patients, pneumococci may cause noninvasive diseases, like otitis and conjunctivitis. In other circumstances, bacteria can travel to the lungs and pass to the blood from there (sepsis), becoming a deadly infection that causes up to 1.5 million deaths per year. The three most lethal pneumococcal infections are pneumonia, invasive sepsis, and meningitis, and they were the cause of the deaths of nearly 1 million children under the age of five in 2017 (https://www.who.int/en/news-room/fact-sheets/detail/pneumonia). In addition to the cost to human lives, pneumococcal infections constitute a heavy economic burden to society (O'Brien et al. 2009). A rough estimate of lower respiratory infections in nearly 200 countries over the years (from 1990 to 2016) gives an impressive number of pneumococcal infections (Troeger et al. 2018). Because of this, understanding the lifestyle of the pneumococcus is important. Among many other important traits, knowledge of pneumococcal TAs is relevant because of their possible participation in colonizing novel niches within the human body that would eventually lead to an infection (Santoro et al. 2019, Colombini et al. 2023).

Bioinformatics and data-mining approaches allowed us to previously propose the possible presence of up to 10 Type II TAs in the genomes of the most relevant strains of *S. pneumoniae* (Chan et al. 2012). Nevertheless, validation and characterization of all the proposed candidates showed that only three TAs were functional in the model strain R6: *relBE*, *yefM-yoeB*, and *pezAT* (Chan et al. 2013). Later on, a fourth *bona fide* functional pair, *phd-doc*, was characterized in the pneumococcal strain Hungary^{19A}-6 (Chan et al. 2014). Finally, the pneumococcal HicA toxin–HicB antitoxin proteins, encoded by strain TIGR4, have been purified and the crystal structure of the HicA–HicB protein complex has been solved (Kim et al. 2018). Although the genetic organization of the operon is *hicA–hicB*, i.e. TA, in all sequenced strains of *S. pneumoniae*, their usual name has been shifted to HicBA (antitoxin–toxin) and as such we shall refer to them from now on (Kim et al. 2018). The toxicity of HicA and its neutralization by the antitoxin HicB was tested in *Escherichia coli* and the RNase activity of the toxin HicA was shown to be high (Kim et al. 2018). We have previously tested the activity of the HicA toxin encoded by the pneumococcal strain Hungary^{19A}-6 (which we have found to be identical to that of strain TIGR4) and it was shown to be inert when tested in *S. pneumoniae* strain R6 (Chan et al. 2014). Whether this discrepancy is due to the different hosts and methods used to perform the toxicity tests is unknown at present.

Considering several of the most representative pneumococcal strains in which their genome sequences are currently available (Inniss et al. 2019, Solano-Collado et al. 2021), we could update the list of verified and possible pneumococcal TAs (Table 1). Out of the four TAs encoded by strain R6, three toxins (RelE, YoeB, and Hic A) would target translation, whereas toxin PezT is the only one with a different target, the cell wall synthesis (Arbing et al. 2010). Bioinformatics analyses of RelBE and YefM–YoeB pairs were performed at the time (Arbing et al. 2010), whereas an in-depth study of the PezAT system has not been performed until now (see below *The PezAT family*).

Genetic organization

The organization of the four pneumococcal operons so far characterized at the genetic and functional levels are typical of Type

Table 1. Some of the relevant strains of *S. pneumoniae* and the TAs they encode.

Strain	HicBA	PhD-Doc	RelBE*	HigBA	YefM–YoeB	PezAT	Total
JJA_1	1	1	2		1	1	6
P1031_1	1	1	3			2	7
AP200	1	1	2		1	1	6
R6	1		2		1	1	5
CGSP14	1	1	2		1	2	7
SP14-BS292		1	3				4
SP3-BS71	1	1	2			1	5
TCH8431/19A	1	1	2				4
BS397	1	1	3		1	1	7
BS455	1	1	3		1	1	7
BS457	1	1	3		1	1	7
BS458	1	1	3		1	1	7
CDC0288-04	1	1	2		1	1	6
CDC1087-00	1	1	2		1	1	6
CDC1873-00_1	1	1	3		1	1	7
GA04375	1	1	1				3
INV200	1	1	2		1	1	5
OXC141	1	1	2			1	5
SP23-BS72		1	2		1	1	5
Taiwan19F-14	1	1	2				4
G54	1	1	2				4
ATCC_700669_1	1	1	3			2	7
CDC3059-06_1	1	1	3		1	1	7
D39	1		2		1	1	5
D39V	1		2		1	1	5
Hungary19A-6	1	1	3		1	1	7
SP11-BS70	1		3		1	1	6
SP14-BS69	1	1	2		1	2	7
SP18-BS74	1	1	3		1	2	8
TIGR4	1	1	3	1			6
ATCC_700669_2	1	1	3		1	1	7
CDC1873-00_2	1	1	3		1	1	7
CDC3059-06_2	1	1	3			1	6
GA41301_2	1	1	3		1	1	7
GA47368_2	1	1	3		1	1	7

*: It includes one copy of the inactive TA previously termed RelBE1 (Chan et al. 2018).

II TAs (Fig. 3): the gene encoding the antitoxin precedes the one encoding the toxin, and both genes overlap by 1–3 nucleotides (nt), which is a strong indication of cotranslation (Woodgate and Zenkin 2023). This was not, however, the case with the *hicBA* operon (see also Fig. 4G), in which 26 nt separate the termination codon of the HicA toxin and the initiation codon of the HicB antitoxin and the two genes are preceded by an open reading frame of unknown function (Chan et al. 2012, Kim et al. 2018). The genetic vicinity of the TA operons varied among different pneumococcal strains, a finding that was remarkably variable in the case of the RelBE pair where up to three different genetic organizations were found in ∼100 clinical isolates, without affecting the promoter of the operon (Nieto et al. 2010). Bioinformatics studies performed at a later stage showed the existence of six different groups of genetic organization in the *relBE* region (Chan et al. 2012). In most cases (designed types A–D strains; Fig. 4), the operon was placed downstream of the *vicX* gene (encoding a metal-dependent hydrolase), and, in two cases, insertion sequences (ISs) were found. In all these strains, we detected the presence of a characteristic 107 nt repeated sequence, termed Repeat Unit of Pneumococcus (RUP) downstream of the *relBE* locus (Figs 4A–D).

RUP elements were considered one of the repeated sequences found in the chromosome of pneumococcus, probably of MGE origin (Croucher et al. 2011). A proposal that RUP sequences may serve as binding sites for regulatory proteins was made (Oggioni and Claverys 1999), and some recent findings on the mechanisms controlling the pneumococcal capsule (*cps*) operon may illustrate their complex roles (Glanville et al. 2023), as follows: the most important virulence trait of the pneumococcus pertains to its capsule, a polysaccharide coat that protects the bacterium from phagocytosis. Around 100 different serotypes have been reported to exist in *S. pneumoniae*, and each one exhibits a different chemical composition in its capsules (Moscoso and García 2009, Ganaie et al. 2020). The *cps* regulon appears to be organized as a single transcriptional unit, with *cpsA* being the first gene of the operon. It exhibits a RUP element upstream of the promoter. The study of the regulatory circuits governing the expression of the capsule showed that two conserved transcription factors, SpxR and CspR, controlled capsule synthesis by binding to a 37-nt distal DNA region named the *37-CE* locus (Glanville et al. 2023). This locus acted *in cis*, and their sequence varied among the pneumococcal serotypes. The analysis of the *37-CE* loci belonging to 87 serotypes showed that their 3′-ends extended within the RUP sequence located upstream of the *cspA* gene (Moscoso and García 2009, Glanville et al. 2023). Whether regulatory proteins would bind to the RUP elements located downstream of the different types of the *relBE* locus and whether they could influence the expression of the upstream genes is presently unknown.

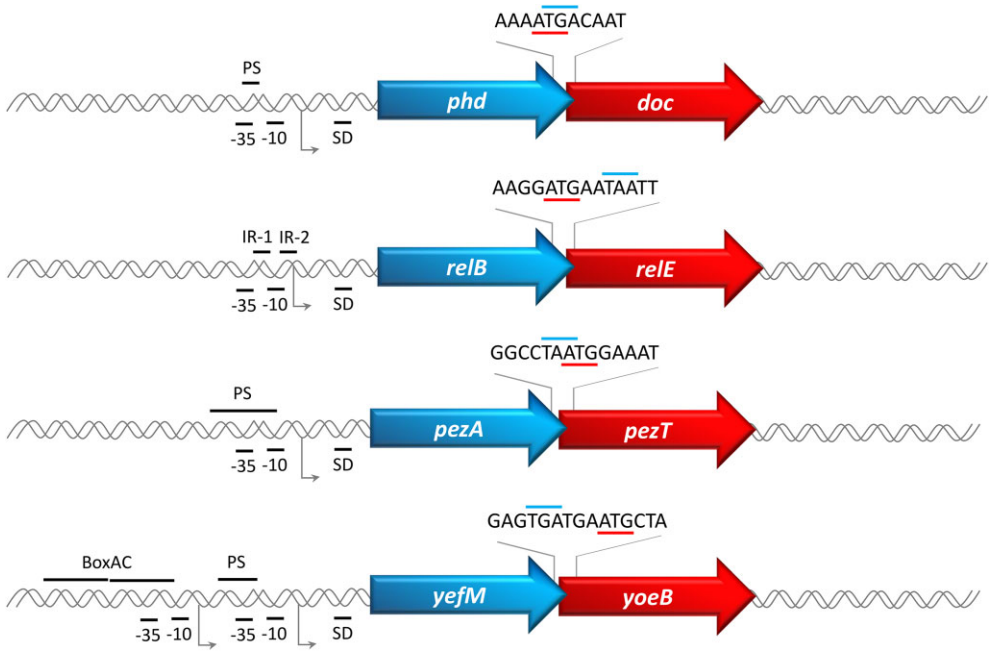

Figure 3. The four best-studied TAs of *S. pneumoniae* are **(A)** *Phd-doc*; **(B)** *relBE*; **(C)** *pezAT*, and **(D)** *yefM–yoeB*. The end codon of the antitoxin gene is underlined in blue, whereas the start codon of the toxin is underlined in red. Preceding the genes, there are located the transcription initiation signals and the targets of the TA pair. PS, palindromic sequence; IR-1 IR-2, inverted repeats; -35 and -10 the regions of the promoter(s), SD, ribosome-binding sites, and BoxAC, the genetic insertion upstream of *yefM–yoeB*.

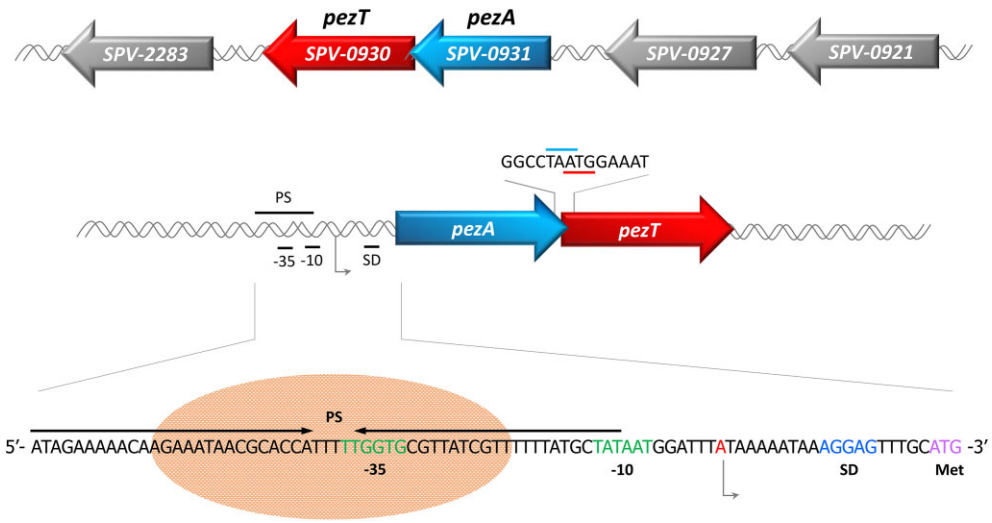

Figure 4. Repeated sequences around the pneumococcal TAs. From (A) to (D), four different gene arrangements of the *relBE* operon are shown, all of them including the RUP element (depicted in green). (E) Shows the intrastrand pairing that would generate a hairpin structure in the BoxAC element located upstream of the *yefMyoeB* and *hicBA* operons. Genes encoding toxins are shown in blue, whereas those encoding toxins are shown in red.

Transcription

The DNA binding sites of the pneumococcal TAs, as determined by DNase I and high-resolution (hydroxyl radical) footprinting experiments (Nieto et al. 2007, Chan et al. 2011, Moreno-Córdoba et al. 2012, 2021), showed the existence of one or two inverted repeats placed within (i) the −10 region and the initiation of the transcription region (*relBE*); ii) the −35 region (promoter 2 of *yefM–yoeB*, and *pezAT* promoter), and (iii) between both regions (*phd-doc*). Upstream and downstream of these TAs, IS elements, genes involved in the mobilization of MGEs, and integrases are located (Chan et al. 2012). We have shown that *relBE*, *pezAT*, and *phd-doc* exhibit a single promoter directing the synthesis of a single mRNA (Nieto et al. 2006, Chan et al. 2014, Moreno-Córdoba et al. 2021). A different organization was observed in the *yefM–yoeB* pair, in which transcription was demonstrated to be directed by two promoters (Chan et al. 2011). In this TA pair, the promoter located more to the 5′-region of the translation initiation codon (Figs 3 and 4F) was generated by the insertion of part of another highly abundant pneumococcal element, termed BOX, which has been found in the chromosome of many pneumococcal genomes (Martin et al. 1992).

BOX elements are inverted repeats that are composed of three modules, termed *boxA* (59 nt), *boxB* (45 nt), and *boxC* (50 nt), or combinations of any of two subelements, or repetitions, especially

of *boxB*, between *boxA* and *boxC*. The *box*AC subelement found in the YefM–YoeB pair (Chan et al. 2012) can fold to yield a stable hairpin (Fig. 4E) that has been shown to influence the expression of genes located downstream of it (Knutsen et al. 2006). The organization of the pneumococcal *yefM–yoeB* operon is different from the *E. coli yefM–yoeB* and the *Enterococcus faecium axe–txe* TAs homologues with the two latter TAs exhibiting a single promoter (Kędzierska et al. 2020). We also found a *box*AC element located 264 nt upstream of the *hicBA* operon and upstream of a putative gene of unknown function (Chan et al. 2012), but whether this particular subelement participates in the regulation of expression of the operon is unknown (Fig. 4G). The function of the pneumococcal *box* element is yet unknown, although it has been postulated to be a mobile sequence that inserts upstream or downstream of certain genes or operons since it has been associated with a putative pneumococcal IS, IS*Spn2* (Knutsen et al. 2006). Insertion of *box* elements upstream of operons could provide new promoters, as in the case of *yefM–yoeB*, whereas downstream insertions could stabilize the mRNA of the operon, as in the competence regulon (Chan et al. 2012, Knutsen et al. 2006).

Functionality

Concerning the roles of the TAs in pneumococcal infections, *relBE* and *yefM–yoeB* deletion mutants exhibited a reduced resistance to oxidative stress and a diminished ability to generate biofilms without affecting cell growth rates (Chan et al. 2018). Both phenotypes were cumulative and the wild-type (*wt*) conditions were partially or fully restored by complementation analyses (Chan et al. 2018). These phenotypes were not observed when the deleted TA was *pezAT* (Chan and Espinosa 2016a). No clear function could be ascribed to the pneumococcal *phd-doc*, but the general features of this particular TA coincided with those defined for the Doc toxin encoded by bacteriophage P1, which is a kinase that inactivates protein synthesis (Cruz et al. 2014). The specific target of Doc toxin remained elusive until it was shown that it belongs to the family of Fic proteins, a conserved group of proteins that participate in many processes through AMPylation of target proteins (Castro-Roa et al. 2013). Inhibition of translation by Doc is performed by phosphorylation of the elongation factor EF-Tu at the conserved Thr382 residue, making it unable to bind aminoacylated tRNAs (Castro-Roa et al. 2013).

The other Type II TAs that were found in *S. pneumoniae*, in particular *hicBA* (Table 1), which encodes another protein synthesis inhibitor toxin, HicA, were present in all the strains analysed (this review and Chan et al. 2012). The three-dimensional structure of the HicB–HicA protein complex was later solved (Kim et al. 2018). In addition to these TAs, there may be at least two more loci encoding solo toxins Ant or Bro, whereas their respective antitoxins might be located elsewhere in the pneumococcal chromosome. Interestingly, these two candidates seemed to be associated with pneumococcal lysogenic prophages. However, to our knowledge, no further molecular experiments have been done on these TAs (Chan et al. 2014). The case of *pezAT* merits a more detailed analysis because (i) contrary to earlier proposals (Mutschler and Meinhart 2013), we have found that it is abundant in bacteria and MGEs (below), and (ii) it exhibits a different mechanism of action than the better-studied RNases.

The *S. pneumoniae pezAT* operon

Among the best-characterized pneumococcal TAs (Table 1), the PezA–PezT pair is most interesting because: (i) it is organized as a single operon, i.e. located within the pneumococcal pathogenicity island 1, PPI1, now renamed ICE*Spn*D39-1 (Liu et al. 2019); therefore, the *pezAT* operon is included within a mobile region (Haudiquet et al. 2022), (ii) PezT (like toxin Zeta, below) targets cell-wall biosynthesis, a feature, i.e. unique to this category of toxins, making them different to other bacterial TAs, (iii) it participates in resistance to β-lactam antibiotics, which are the routinely used drugs in the treatment of pneumococcal diseases (Chan and Espinosa 2016b), and (iv) depending on the strains, there may be a second copy of the operon in the chromosome. The name of this TA pair is derived from pneumococcal epsilon zeta, the Epsilon–Zeta TA homologue encoded by the streptococcal plasmid pSM19035 that was earlier characterized in depth (Ceglowski et al. 1993, Lioy et al. 2012, Moreno-del Álamo et al. 2019). The structures of both protein pairs have been solved (Meinhart et al. 2003, Khoo et al. 2007), and the interactions of the PezA–PezT complex with their target DNA have been defined (Khoo et al. 2007).

Genetic organization

In the chromosomes of the *S. pneumoniae* strain D39, as well as in the deep-genome annotated strain D39V (Slager et al. 2019), and in the derivative R6 strain (Tettelin et al. 2001), a single copy of the *pezAT* operon (NCBI accession numbers CP027540.1 and NC_003098, respectively) was found (Fig. 5A). The operon is located at the complementary strand between coordinates 1021730–1022206 (*pezA*) and coordinates 1020969–1021730 (*pezT*). This region is included within ICE*Spn*D39-1, an Integrative and Conjugative (mobile) Element from *S. pneumoniae* (Liu et al. 2019). As in the case of the other pneumococcal TAs, the operon is surrounded by MGEs indicative of a high variability among strains, not only in size but also in the genes included in the region (García 2023). We have found that other pneumococcal strains, for instance, CGSP14, ATCC700669, and P1031 have two copies of the same operon (Chan et al. 2012; Table 1). Transcription of the operon is directed by a single promoter, P_{AT} (Fig. 5B) and the PezA–PezT protein complex binds to a long palindromic sequence spanning the entire promoter, although the two proteins bind to the −35 region of the promoter (Fig. 5C). Differently from the Epsilon–antitoxin, PezA alone could play a regulatory role, which is less strong than the PezA–PezT complex (Khoo et al. 2007). Upon binding to DNA, the PezA–PezT protein complex would inhibit the binding of the host RNA polymerase to its target DNA, although, to our knowledge, no DNA bending induced by the binding of the proteins to their target has been tested (Chan and Espinosa 2016a). Prediction of possible curvatures on the DNA helix in a sequence encompassing the region upstream of and the P_{AT} promoter (Fig. 6A) showed two regions with the potential to be curved (Fig. 6B). We anticipate that the binding of the PezA–PezT protein complex would induce a bend around this region, which would hinder the binding of the host RNA polymerase to the promoter, as was the case with the CopG protein encoded by plasmid pMV158 (Hernández-Arriaga et al. 2009).

Structures of the PezA–PezT and epsilon–zeta protein complexes

The crystal structure of the $PezA_2$–$PezT_2$ heterotetramer complex was solved (Khoo et al. 2007). The three-dimensional structure (Fig. 7; PDB: 2P5T) is such that a PezA–PezT unit is mirrored by a vertical axis to another unit so that the resulting heterotetramer is composed of two PezA molecules that sandwich two PezT molecules, yielding a tight complex that occludes the active site of the PezT molecules. Whereas the usual affinity of the TA

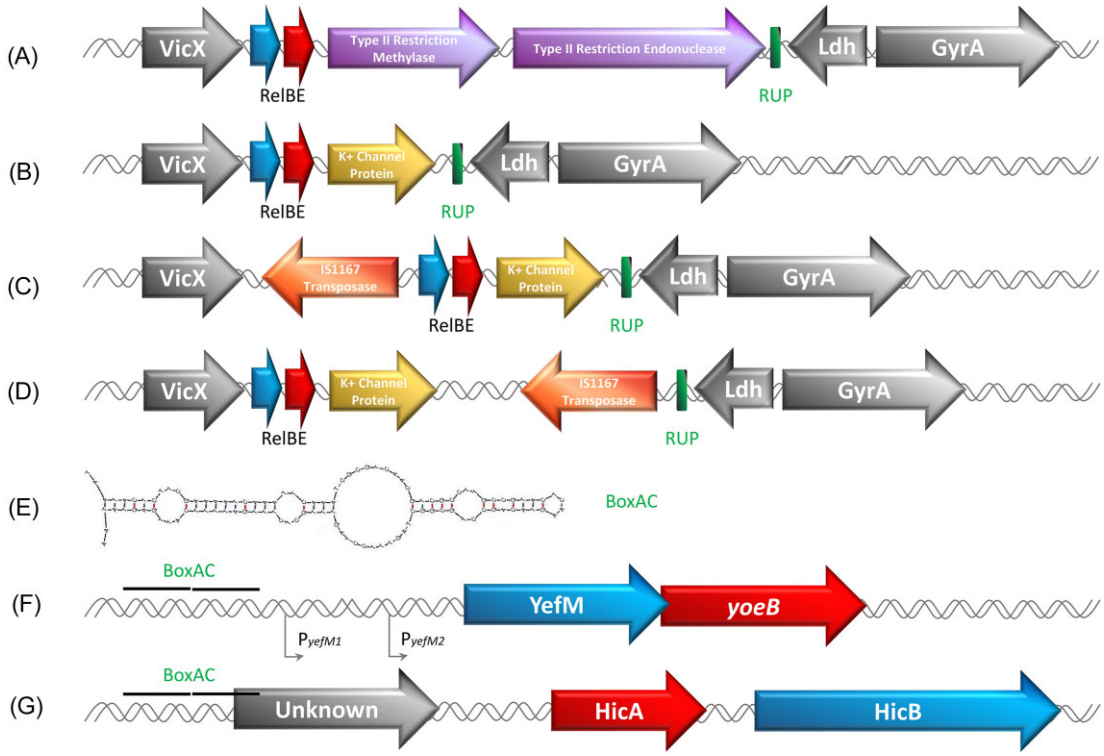

Figure 5. Genetic organization of the *pezAT* operon in the S. *pneumoniae* strain R6 chromosome. (A). The TA pair is embedded within the PP1I pathogenicity island and is encoded on the complementary strand. (B). The TA pair is transcribed from a single promoter, P_{AT} and both genes seem to be translationally coupled. (C). Proteins PezA and PezT bind as a heterotetramer (ellipse) to a long inversely repeated sequence (indicated by arrows) that encompasses the entire promoter. The initiation of transcription is indicated by a grey arrow below the A initiation point; the −35 and −10 boxes of the promoter (green), and the ribosome binding site (SD, blue), are shown. The first (Met) codon is marked (cyan).

protein complexes lies in the nanomolar range, the affinity of PezA for PezT is in the femtomolar range, being one of the strongest affinity values reported (Mutschler et al. 2010). The *in vivo* and *in vitro* stabilities of the epsilon–zeta and PezAT protein complexes have been analysed in detail (Camacho et al. 2002, Mutschler et al. 2010).

Comparison with the structure of the epsilon$_2$–zeta$_2$ complex (Meinhart et al. 2001, 2003) showed that the structures of both TA complexes (PezA–PezT and epsilon–zeta) are similar. The antitoxins Epsilon and PezA have a similar fold of three α-helix bundles. However, PezA (158 amino acid residues) is larger than Epsilon (90 residues) and both proteins are homologous at their C-terminal moiety only. This difference may be due to PezA exhibiting a helix-turn-helix (HTH) DNA-binding motif (Pabo and Sauer 1984), at its N-terminal moiety (Khoo et al. 2007, Mutschler and Meinhart 2013). The HTH motif of PezA is involved in its binding to the long palindromic sequence located on the promoter of the TA pair (Fig. 5), and the control is reinforced by the binding of the toxin PezT that acts as a corepressor (Khoo et al. 2007). The tripartite omega–epsilon–zeta proteins have a more complex organization. Omega is a general transcriptional repressor encoded by plasmid pSM19035 that controls, among other genes, the synthesis of the polycistronic *omega–epsilon–zeta* mRNA (de la Hoz et al. 2004). Omega belongs to the ribbon-helix-helix (RHH) family (Murayama et al. 1999, 2001) and binds cooperatively as a dimer to different promoters on the plasmid, with 7–10 consecutive non-palindromic heptad repeats (de la Hoz et al. 2000, 2004, Weihofen et al. 2006). Interestingly, a homologue of PezAT, termed PezAT^{Mtb}, has been found in *M. tuberculosis* but the antitoxin belongs to the RHH family (Tandon et al. 2019).

Concerning the toxins, both, PezT and Zeta are folded like a phosphotransferase: one Walker A motif for the binding of ATP or GTP and a phosphoryl-transferase active site, whereas both antitoxins (PezA and Epsilon) hinder the toxicity of their counterparts by occluding their active sites (Meinhart et al. 2003, Khoo et al. 2007). The similarities of the structures of Epsilon–Zeta and PezA–PezT are such that some cross-reactivity has been found between them: Epsilon antitoxin interacted with PezT toxin and could partly alleviate its toxic effect; conversely, the toxicity of Zeta toxin could be also relieved by the PezA antitoxin (CCY, unpublished observations). Site-directed mutagenesis performed at residues of PezT that are also conserved in Zeta showed that, in both cases, toxicity was lost (Khoo et al. 2007).

Toxicity of PezT

The roles of epsilon–zeta proteins and further details concerning their relevance have been recently analysed in-depth (Moreno-del Álamo et al. 2019, 2020; and references therein), and thus, we shall not pursue this tripartite-TA further. The toxic effect of PezT was assayed in *E. coli* and it was shown that overproduction of the toxin resulted in cell growth arrest for as long as 180 min, but growth could be restored by synthesis of the PezA antitoxin (Khoo et al. 2007), indicating that only overproduction of the toxin could be lethal. Later on, it was found that expression of a PezT truncated protein (lacking the last 11 residues) resulted in membrane permeabilization followed by cell lysis (Mutschler et al. 2011). This led to the characterization of PezT as an inhibitor of cell wall synthesis by phosphorylation of the uridine-diphosphate-*N*-acetylglucosamine (UNAG) to UDP-*N*-acetylglucosamine-3´-phosphate

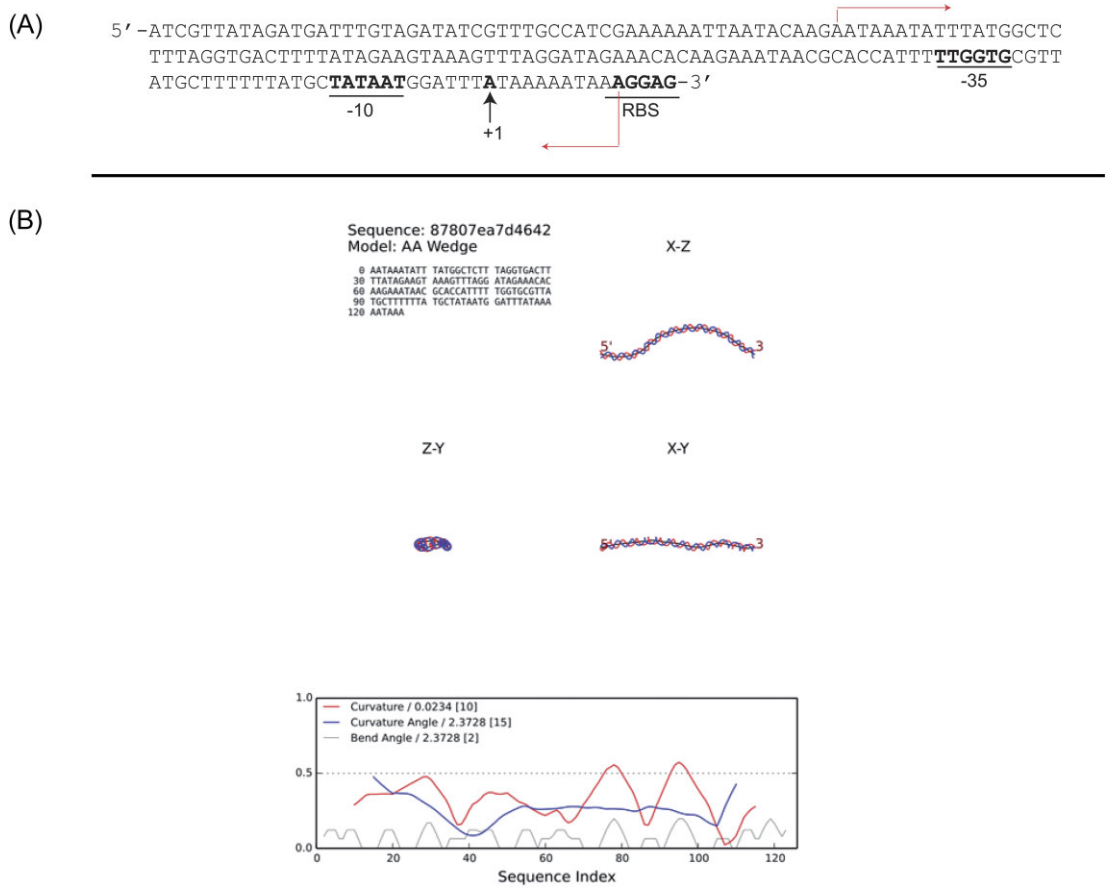

Figure 6. Predicted intrinsic curvatures upstream of and around the P_{AT} promoter region. (A) The DNA region used to perform the predictions includes the entire promoter and it is shown encompassed by the two red arrows. The −35 and −10 boxes of the promoter (boldface letters, underlined), the transcription initiation point (vertical black arrow), and the ribosome binding site (RBS) are indicated. (B) Two different programs were used to perform the predictions: (i) CURVES+ (https://bioinformaticshome.com/tools/nucleic acid-structure-analysis/descriptions/CURVES + .html), which predicts curved regions on the three spatial axes (upper part) (Blanchet et al. 2011) and (ii) BEND.IT (http://pongor.itk.ppke.hu/?q=bioinfoservices), which predicts DNA curvatures from DNA sequences (lower panel). In both cases, two regions exhibiting potential DNA curvatures were predicted.

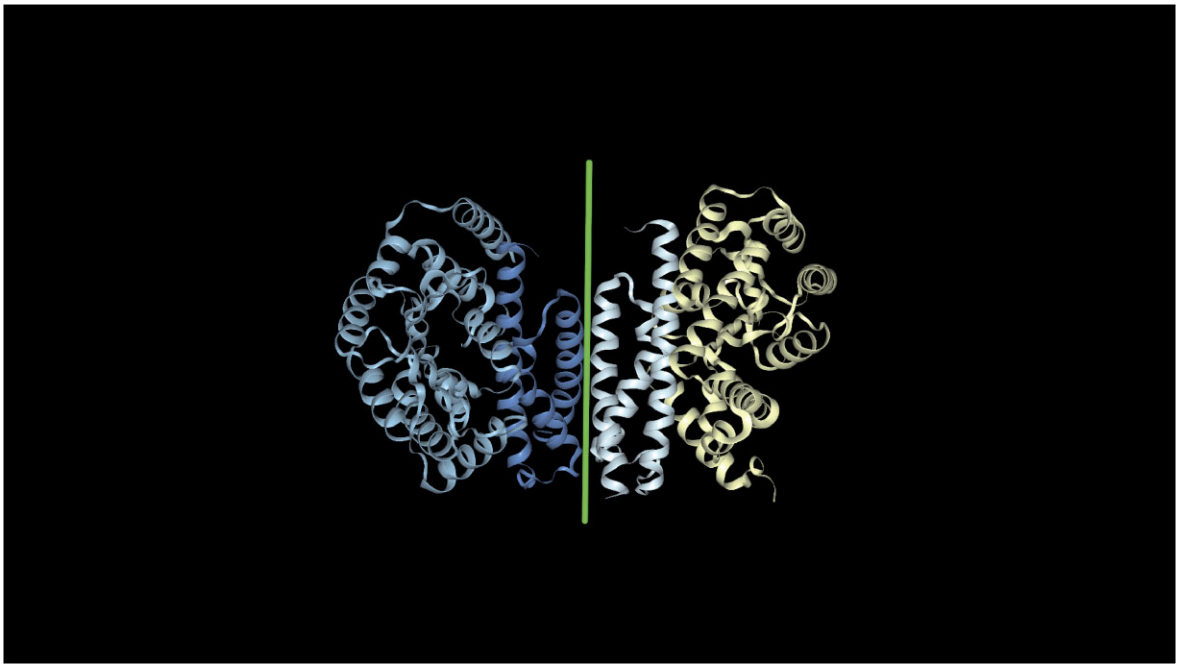

Figure 7. Screen-shot of the PezAT tetramer structure composed of two dimers (PDB: 2P5T; https://www.rcsb.org/structure/2P5T; Khoo et al. 2007). The symmetry axis is drawn in green.

(UNAG-3P) in the presence of ATP and Mg^{2+}. UNAG is produced in the hexosamine biosynthetic pathway and is essential for bacterial cell wall peptidoglycan biosynthesis. Accumulation of UNAG-3P in the cellular cytosol competitively hinders the catalytic activity of the MurA protein, which is essential in the initial steps of peptidoglycan synthesis, thus compromising the entire pathway and resulting in cell death (Mutschler et al. 2011).

Roles of PezAT in the pneumococci lifestyle

The *pezAT* operon was found to be absent in various clinical isolates of *S. pneumoniae* (Khoo et al. 2007). The toxin PezT was proposed to be associated with the virulence of this bacterium because a strain deleted in the *pezT* gene was found to have reduced infectivity in mice, without being affected by its cellular growth (Brown et al. 2004). These results agree with the reported increased expression of *pezT* in conditions mimicking lung infections in mice (Aprianto et al. 2018). Furthermore, pneumococcal serotype 1 strains were analysed and it was found that the *pezAT* operon was located within the variable region of ICE*Spn*D39-1 in all hypervirulent isolates, but the operon was absent in strains with low or medium invasive ability, pointing to an important role of the hypervariable regions in the pneumococcal diseases (Harvey et al. 2011). These findings are not surprising because of the high recombination rate exhibited by the natural competence of *S. pneumoniae* (Hanage et al. 2009). A possible contribution of PezT to virulence was envisaged because the toxin would trigger cell lysis with the concomitant release of pneumolysin, a major virulence factor that increases the progress of infection (Mutschler et al. 2010, 2011). Partial autolysis would lead to the release of chromosomal DNA, which could increase biofilm formation, another contributor to virulence (Mutschler et al. 2011). Interestingly, a recent report has shown that extracts from *Lawsonia inermis*, a medicinal plant used in Indonesia, exhibited a potent antipneumococcal activity by producing bacterial lysis, antibiofilm activity and cell-wall disruption by the increase of the synthesis of *lytA* (the major pneumococcal autolysin) and, curiously, a decrease in *pezAT* expression (Tafroji et al. 2022).

In our case, however, we found that deletion of the *pezAT* operon in the pneumococcal strain R6 (in which exists a single copy of the TA pair), did not lead to detectable changes in two virulence-related parameters: (i) biofilm formation, and (ii) sensitivity to oxidative stress (Table 2). Further, there were no significant changes in the growth of the strains during the exponential phase (Table 2), although the deletion mutant showed an enhanced resiliency to lysis at the stationary phase and the cell chains were shorter than those of the *wt* strain (Chan and Espinosa 2016a). We also observed that deletion of the *pezAT* operon resulted in a moderate (2-fold) increase in the resistance to β-lactam antibiotics and an increase in the transformability levels (Fig. 8). We concluded that a balance between two gains of functions, i.e. an increment in the resistance to β-lactam antibiotics, and an increase in transformability, could compensate for a loss of function, like the reduction of virulence. Very preliminary studies (WTC and ME, unpublished) compared the transcriptome of the *wt* strain with that of the deleted derivative, both strains grown in conditions that maximize the bacterial onset in the competent state. The results indicated that the deleted strain substantially incremented the expression of the *lytB* gene, which encodes another pneumolysin essential for cell separation (García et al. 1999). It has been shown that the protein LytB is essential for the adhesion and invasion of *S. pneumoniae* into the epithelial cells of the human lungs (Bai et al. 2014) as well as for biofilm formation

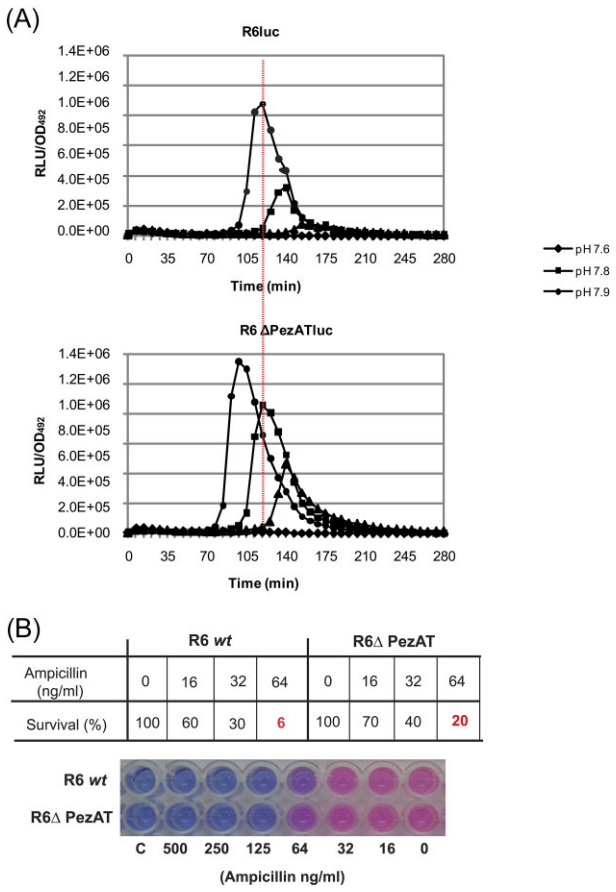

Figure 8. Competence development and resistance to ampicillin in *S. pneumoniae*. A new strain of *S. pneumoniae* R6 was constructed by the insertion of a single copy of a transcriptional fusion of the promoter of the *ssbB* gene (a late competence gene) and the *Photinuspyralis luc* gene (encoding firefly luciferase) followed by a chloramphenicol resistance gene (Chan and Espinosa 2016b). (A) Deletion of the *pezAT* operon increases genetic competence. The development of spontaneous competence of both pneumococcal *wt* and Δ*pezAT* mutant cells was assessed by measuring, at different pHs, the transcriptional level of the *luc* gene. Values depicted are Relative Luc Units (RLU) measured at OD_{492}, at the indicated pH. The vertical line joining both panels points to the time differences in the onset of the main peaks of competence. (B) Deletion of the *pezAT* operon increases resistance to ampicillin, which was measured as the percentage of surviving cells at the concentrations of antibiotic tested and as strain-resistances detected by MIC, determined by the change of colour from resazurin (blue) to resorufin (pink).

(Domenech and Garcia 2020). Nevertheless, all the above information is, in our opinion, insufficient to attain a direct relationship between PezAT and virulence.

The PezAT family of proteins

The epsilon–zeta pair encoded by plasmid pSM19035 was initially presumed to be restricted to G+ bacteria, especially streptococci (Meinhart et al. 2003), and a similar situation was reported for the PezAT family (Khoo et al. 2007). However, it was later discovered that homologues of this module were distributed among bacterial phyla, although their abundance seemed to be small (Leplae et al. 2011, Mutschler and Meinhart 2013). Two of these TAs were found to exist in G− bacteria, namely *E. coli* (EzeT) and ng_ε1/ng_ζ1 from *Neisseria gonorrhoea* (Rocker and Meinhart 2015, Rocker et al. 2018). In the case of EzeT, the antitoxin and toxin are encoded in the

Table 2. Deletion of the *pezAT* operon does not affect pneumococcal growth at the exponential phase, biofilm formation, or oxidative stress.

Strain/plasmid	Growth (OD_{595})	Growth (%)	Biofilm[a]	Biofilm (%)	CFU[b] per plate (No H_2O_2)	CFU per plate (20 mM H_2O_2) and survival (%)	CFU per plate (40 mM H_2O_2) and survival (%)
R6 wt/none	0.347	100	3.744	100	307 (100)	160 (52.1)	107 (34.8)
R6 wt/pC194r	0.300	86	3.877	104	301 (100)	148 (49.2)	110 (35.5)
Δ*pezAT*/none	0.342	99	3.884	104	310 (100)	156 (50.3)	118 (38.1)
Δ*pezAT*/pC194r::*pezAT*	0.302	87	3.961	106	298 (100)	157 (52.7)	114 (38.2)

[a]Biofilm formation capacity of the following strains of *S. pneumoniae* R6: wild type (wt), wt harbouring the low copy-number plasmid pC194r, Δ*pezAT*, and Δ*pezAT* harbouring plasmid pC194r in which the *pezAT* operon was cloned. Growth and biofilm formation were performed as described (Moscoso et al. 2006 , Chan et al. 2018). The measured values were normalized for the controls (no cells) and the percentages were calculated related to the values obtained for the wt strain. The results are the average of three independent experiments.

[b]Pneumococcal cultures at OD_{650} ~0.3 were treated with H_2O_2, 20 min, 37ºC, and the surviving cells were determined by counting the number of colony-forming units per ml (CFU/ml) on plates (Chan and Espinosa 2016b). The results are the average of four independent experiments.

same polypeptide, the N-terminal corresponding to the antitoxin and the C-terminal to the toxin moiety (Rocker and Meinhart 2015). EzeT exhibits a lytic phenotype that was attributed to UDP-*N*-acetylglucosamine phosphorylation. The gonococcal TA is organized as an operon and purification of the two proteins allowed to demonstrate that the ng_ε1 antitoxin has a fold, i.e. unrelated to the cognate epsilon antitoxins, whereas the ng_ζ1 Zeta toxin displays a wider specificity of the substrate, being able to phosphorylate multiple precursors of peptidoglycan synthesis, perhaps as a reflection of the different composition in the cell-wall of G+ or G− bacteria (Rocker et al. 2018). Also, in contrast to the canonical zeta toxins, ng_ζ1 phosphorylates UDP-activated sugars at the C4′-OH group of the hexose moiety.

The omega–epsilon–zeta system encoded by the streptococcal plasmid pSM19035 was shown to stabilize a segregationally unstable plasmid in the heterologous host *Bacillus subtilis* (Ceglowski et al. 1993) although, to our knowledge, it was never tested in the host where the plasmid was originally isolated, *S. pyogenes* (Behnke et al. 1979). Much more recently, three plasmids from glycopeptide-resistant *E. faecium* (pVEF1, pVEF2, and pVEF3) were each shown to harbour a functional omega–epsilon–zeta-type TA system that was able to stabilize the segregationally unstable enterococcal plasmid pAT18 in *E. faecalis* OG1X, although with decreasing effect over time (Sletvold et al. 2008). The omega–epsilon–zeta system of pVEF1/pVEF2 was more efficient in plasmid maintenance in *E. faecalis* than the homologous TA system on pVEF3. Amino acid and nucleotide sequence analysis showed that the epsilon–zeta proteins encoded by pVEF1/pVEF2 had higher identity scores to the epsilon–zeta counterparts encoded by pSM19035, whereas pVEF3 is identical to pRE25 (Sletvold et al. 2008), a plasmid also of the *Inc*18 family and isolated from *E. faecalis* RE25 (Schwarz et al. 2001). The amino acid sequence identities of the omega–epsilon–zeta proteins from pVEF3 and pSM19035 ranged between 96% and 100% (Sletvold et al. 2008). The omega binding site and the promoter of the operon are identical in pVEF1/pVEF2 and pVEF3 indicating that neither regulation nor transcriptional differences would be responsible for the different ability of plasmid maintenance in *E. faecalis* OG1X (Sletvold et al. 2008). However, we have to take into account that the Omega protein from plasmid pSM10035 has been shown to switch from repression to activation by interacting directly with the *B. subtilis* RNA polymerase, a situation that, to our knowledge has not been tested for the enterococcal plasmids (Volante et al. 2015).

We performed an in-depth search for the conservation of the PezA–PezT proteins, taking into account that among the TA pairs, it is always the toxin partner, i.e. more conserved. The global search for the presence of the PezT/Zeta toxin homologues was performed using the NCBI RefSeq212 dataset of plasmids and bacteria (accessed October 2022). The dataset was inspected with the Pfam HMM profile (Zeta_toxin, PF06414.15) (Mistry et al. 2020) by using the *hmmsearch* function of HMMER 3.1b2 (Eddy 2009) (parameters –incE 10^{-10} –incdomE 10^{-10}). A total of 3086 homologues with ≥ 80% HMM profile coverage were retrieved, whereby 2358 homologues were located in chromosomes and 728 in plasmids (Table S1, Supporting Information). These findings are indicative of a much broader distribution of PezT in bacteria than previously suspected. The diversity of the PezT/Zeta-like proteins is illustrated in the maximum-likelihood phylogenetic tree shown in Fig. 9. They are distributed among 14 bacterial phyla, mostly in Proteobacteria (48%), Firmicutes (27%), and Actinobacteria (18%). PezT/Zeta-like proteins encoded either on chromosomes or plasmids are intermingled along the tree. Nevertheless, clades are generally populated, at short evolutionary distances, with members encoded in one of these genome types, although some instances of mixing can be distinguished. To estimate recent horizontal transfer events of the *pezT/zeta* genes between chromosomes and plasmids, the PezT/Zeta-like proteins were clustered when exhibiting at least 99% identity and 95% coverage, using MMseqs2 (Steinegger and Söding 2017). 755 PezT/Zeta clusters were obtained, 206 of which contained at least two proteins (Table S2, Supporting Information). Of these, only 11 clusters contained members occurring in both genome types, in some instances in different strains of the same or different species, while others within the same isolate. These mixed clusters are indicative of the recent movement of these TA systems between plasmids and chromosomes.

The *pezT*-encoding genomes were, in turn, searched with the Pfam HMM profiles of the antitoxins PezA (HTH_3, PF01381.25) and Epsilon (Epsilon_antitox, PF08998.14), and the Omega regulator (Omega_Repress, PF07764.14). Hits obtained with the above-mentioned thresholds of E-value and coverage, and located contiguous to a *pezT/zeta* gene are recorded in Table S1 (Supporting Information). A subset of PezT/Zeta was found to be associated either with PezA or epsilon/omega homologues, but not with both at the same time. With some exceptions, such associations are not dispersed in the tree but occur in specific clades (Fig. 9). This suggests that only closely related PezT/Zeta homologues share the same antitoxin type. Interestingly, 286 PezA homologues were associated with PezT/Zeta-like, out of which 282 were in chromosomes and rarely in plasmids (just four). The placement of these canonical plasmid-encoded PezAT-like systems scattered in a phylogenetic clade predominantly populated by chromosomal PezAT (Fig. 9) is suggestive of *pezAT* acquisition by plasmids from chromosomes. Most canonical PezAT systems are encoded

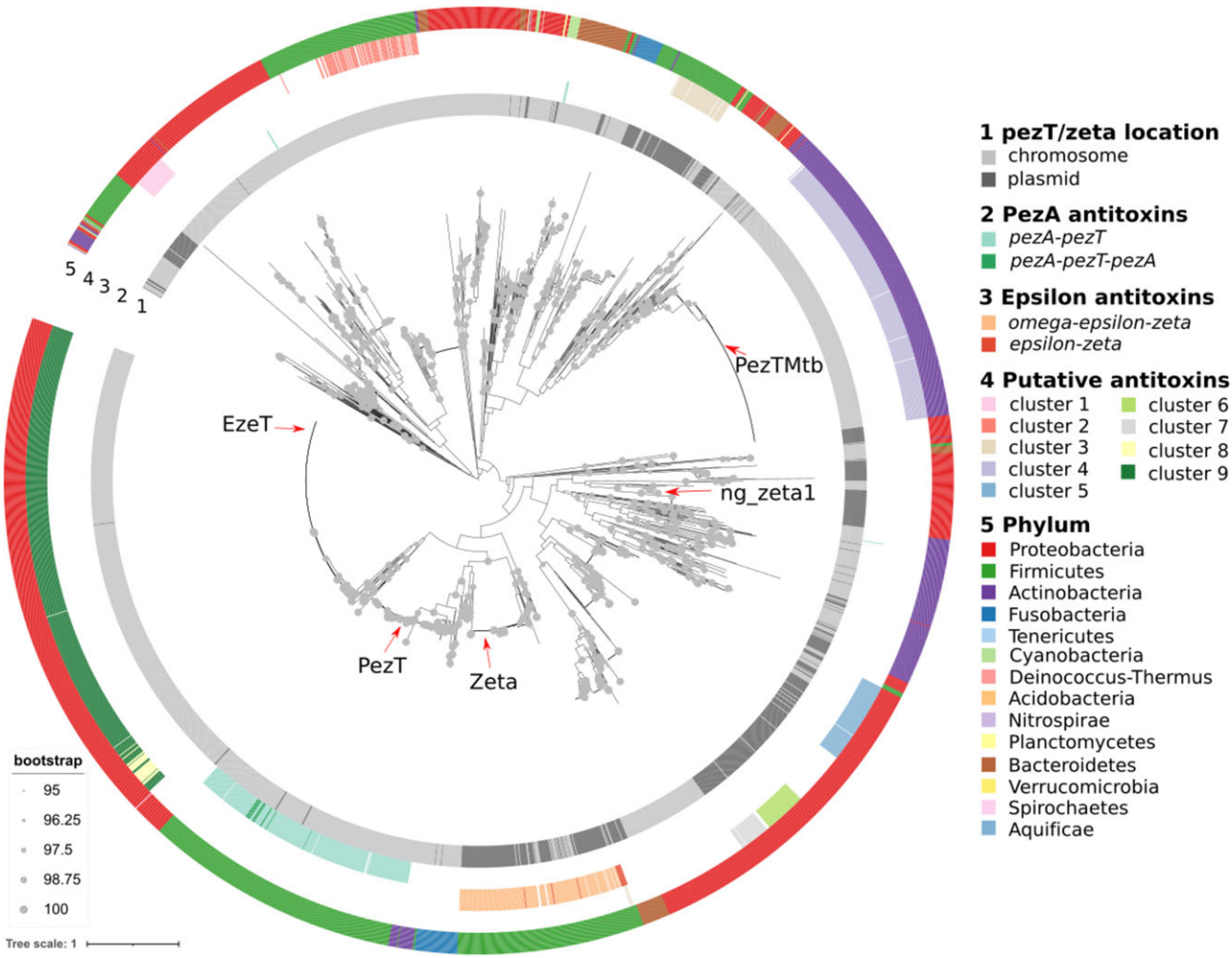

Figure 9. Phylogenetic tree of PezT/Zeta-like proteins. Sequences were aligned with MUSCLE v3.8.3 (Edgar 2004). Positions in the alignment with gaps in 20% or more of the sequences were removed with TrimAl 1.2rev59 (Capella-Gutiérrez et al. 2009). The maximum likelihood phylogeny was inferred with IQ-TREE 1.6.1 (Nguyen et al. 2014), using the VT + F + R9 model of substitution selected with ModelFinder (Kalyaanamoorthy et al. 2017). Branch support was obtained with the ultrafast bootstrap (UFB) approximation (Hoang et al. 2017), and nodes supported with UFB values ≥ 95% are indicated by a circle. The tree was rooted using the midpoint criterion and visualized with iTOL (Letunic and Bork 2019) (https://itol.embl.de/). Five rings surround the tree and are coloured according to the legend at the right. From inward to outward: (1) genomic location of the *pezT/zeta* genes, (2) presence of PezA antitoxin, (3) presence of epsilon antitoxin, (4) clusters of homologous proteins encoded immediately upstream of the *pezT/zeta* gene, and (5) phylum of the bacteria encoding *pezT/zeta* genes. Red arrows point to PezT/Zeta homologues that are members of *bona fide* TA systems with experimental validation: the dual TA EzeT (WP_000212693.1), PezT (WP_000405357.1) of the pneumococcal PezAT system, Zeta (WP_001284311.1) of the omega–epsilon–zeta system, ng_ζ1 (WP_003401859.1) of the ng_ε1/ng_ζ1 system, and PezT^{Mtb} (WP_003401859.1) of the PezAT^{Mtb} system.

in Firmicutes (270), with a few examples in Actinobacteria (10), Bacteroidetes (3), and Proteobacteria (2). On the other hand, 180 PezT/Zeta-like were associated with omega–epsilon and 10 only with epsilon (with no Omega regulator detected). Epsilon-like antitoxins are enriched in plasmids (156 homologues) and only a few are found in chromosomes (34), all of them from different families of the phylum Firmicutes (Fig. 10). PezT/Zeta-like toxins associated with Epsilon antitoxins are clustered in the same phylogenetic clade (Fig. 9), being the more ancestral traits encoded in plasmids, which suggests *omega/epsilon/zeta* system acquisition by chromosomes from plasmids, in direct contrast to the *pezAT* system.

As shown in the tree, several PezT/Zeta homologues do not have a cognate PezA or Epsilon antitoxin (Fig. 9). Following the 'guilt by association' principle (Makarova et al. 2009), putative novel antitoxins of these orphan PezT/Zeta toxins were searched. Genes encoded upstream of these *pezT/zeta* were selected and their protein products were clustered with MMseqs2 (Steinegger and Söding 2017) at 80% identity and 80% coverage. Table S3 (Supporting Information) records the nine clusters with more members, which are depicted in ring 4 of Fig. 9, leaving out those containing PezA or Epsilon antitoxins. Four of these clusters matched a Pfam family with Evalue $\leq 10^{-10}$ and HMM profile coverage ≥ 80%: cluster 1 (PF04962.15, KduI, 5-deoxy-glucuronate isomerase), cluster 4 (PF11903.11, ParD_like, hypothetical protein), cluster 8 (PF08765.14, Mor, DNA-binding protein), and cluster 9 (PF00696.31, AA_kinase, lysine-sensitive aspartokinase 3). Cluster 4 includes the antitoxin of the non-canonical PezAT system Rv0366c–Rv0367c, which is the aforementioned PezAT^{Mtb} system described and functionally characterized in *M. tuberculosis* in which the PezAMtb antitoxin contains an RHH-fold (Tandon et al. 2019). Interestingly, this non-canonical PezAT^{Mtb} appeared to be restricted to the phylum Actinobacteria (Fig. 9), where it has been previously reported to be confined mainly to the family Mycobacteriaceae, 124 reported (Tandon et al. 2019). The lysine-sensitive aspartokinase 3 ho-

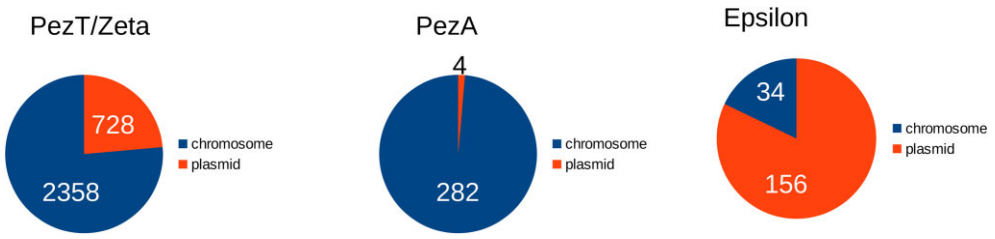

Figure 10. Distribution of toxins (PezT, Zeta) and antitoxins (PezA, Epsilon) homologues in bacterial chromosomes (blue) and plasmids (red).

mologues in cluster 9 were reported near the dual antitoxin–toxin protein EzeT in *E. coli* B1 strains (Rocker and Meinhart 2015).

There is currently a lack of experimental knowledge on PezT/Zeta homologues that do not belong to the canonical PezAT or omega–epsilon–zeta systems. Only in a few instances these homologues, each belonging to a different phylogenetic clade as indicated by arrows in Fig. 9, have been researched. First, there is experimental evidence for the EzeT toxin, which consists of two domains combining toxin and *cis*-acting antitoxin functionalities in a single protein (Rocker and Meinhart 2015). The C-terminal part of the gene product was identified to contain a Zeta toxin domain with 38% and 47% aa similarity to Zeta and PezT, respectively. EzeT exhibits a lytic phenotype that was attributed to UDP-*N*-acetylglucosamine phosphorylation, and the presence of the N-terminal antitoxin domain inhibits EzeT toxicity *in vivo* and strongly attenuates kinase activity. A second example is the ngε_1/ngζ_1 TA system, encoded in a plasmid in *N. gonorrhoea* (Rocker et al. 2018). The ngζ_1 toxin is located in a phylogenetic clade more distantly related to the toxins of the PezAT, omega–epsilon–zeta, and EzeT systems (Fig. 9). As stated earlier, and in contrast to the canonical zeta toxins, the ngζ_1 toxin phosphorylates UDP-activated sugars at the C4′-OH group of the hexose moiety. It also displays broader substrate specificity and phosphorylates multiple UDP-activated sugars that are precursors of peptidoglycan and lipopolysaccharide synthesis. In ngζ_1, the P-loop motif is located much closer to the C-terminus when compared with streptococcal PezT/Zeta toxins whereas the ngε_1 antitoxin has no similarities to any known Epsilon protein (Rocker et al. 2018). Third, the PezAT^{Mtb} system of *M. tuberculosis* (Tandon et al. 2019), whereby the PezT^{Mtb} toxin is located in a phylogenetic clade even more distantly related to the toxins of the PezAT, omega–epsilon–zeta, EzeT, and ngε_1/ngζ_1 systems (Fig. 9). PezT^{Mtb} harbours the antitoxin-binding arginine residue (at position 116) and an aspartate residue (at position 36) that prepares the substrate for phosphorylation through deprotonation, and the P-loop motif for NTP binding. However, the amino acid residues of Zeta and PezT toxins that bind to known substrates such as UNAG are not conserved in PezT^{Mtb} (Tandon et al. 2019). The functional target of this mycobacterial PezT homologue has yet to be identified. When overexpressed, PezT^{Mtb} induces bacteriostasis, reduces cell length, and increases tolerance of the heterologous *M. smegmatis* host to ethambutol (a cell wall inhibitor) *in vitro*. Besides, this growth inhibition was restored by coexpressing *pezT*^{Mtb} along with the predicted antitoxin partner *pezA*^{Mtb}, which, unlike canonical PezA antitoxins, contains an RHH motif (Tandon et al. 2019). It is thus difficult to reliably infer similar functions at large evolutionary distances but these three examples, scattered in different phylogenetic clades of the PezT/Zeta-like tree, suggest that out of the well-known PezAT and omega–epsilon–zeta systems, other homologues of PezT/Zeta do form noncanonical PezT/Zeta-like TA systems that are also functional and likely target the cell wall.

The relationships between the 706 plasmids encoding *pezT/zeta*-like genes were evaluated by calculating the average nucleotide identity (ANI) between all plasmid pairs, as described (Redondo-Salvo et al. 2020). Figure 11 shows the resulting network in which *pezT/zeta*-encoding plasmids are represented by nodes that are connected when they meet the ANI_{L50} score requirements (Redondo-Salvo et al. 2020). A total of 165 groups were obtained, of which 11 contained at least 10 members mostly present in the same phylum (Fig. 11A; Table S4, Supporting Information). They gathered plasmids with similar genomes. We then used COPLA (Redondo-Salvo et al. 2021) to classify the plasmids in plasmid taxonomic units (PTUs), an equivalent to molecular species (Redondo-Salvo et al. 2020). 36 PTUs were identified in the dataset and 303 plasmids were assigned to a PTU (Table S4, Supporting Information), highlighting the diversity of the *pezT/zeta*-encoding plasmids. For most of these plasmids, a known cognate antitoxin is absent (Fig. 11B). Most plasmids encoding an *omega–epsilon–zeta* system showed association in the network, i.e. they keep high overall genome similarity. It likely indicates the acquisition of this system by the ancestral plasmid backbone of this group. Nevertheless, there are also instances of disconnected *omega–epsilon–zeta* nodes, as is also the case for *pezA*-encoding plasmids, suggesting that the *omega–epsilon–zeta* and *pezAT* systems have been independently acquired by different plasmid genomes. A total of 539 out of 706 plasmids encoded a MOB relaxase (Fig. 11C), of which 319 also encoded a mating pair formation (MPF) system (Fig. 11D), indicating that a significant portion of the *pezT/zeta*-encoding plasmids are transmissible by conjugation. A total of 251 plasmids of this dataset also encode antimicrobial resistance genes (Table S4, Supporting Information).

Conclusions and perspectives

The success of bacterial populations, measured by their growth and colonization ability, will strongly depend upon the environment they inhabit. In general, bacterial communities usually install as multispecies biofilms in which sessile individuals constitute the main group. However, some planktonic cells ('explorers'), may release themselves from the main biofilm matrix and seek novel niches where they can establish new colonies. During these colonization attempts, bacteria are frequently subjected to environmental fluctuations in their new niches, like nutrient limitations or overabundance, changes in temperature, salinity, or pHs, i.e. the so-called 'feast or famine' response (Suarez-Mendez et al. 2014). To cope with these changes, bacteria trigger sets of specific transcription proteins that activate or repress several operons involved in their survival, which we have termed the *nichome* (Bravo et al. 2018). While colonization of new niches frequently ends in

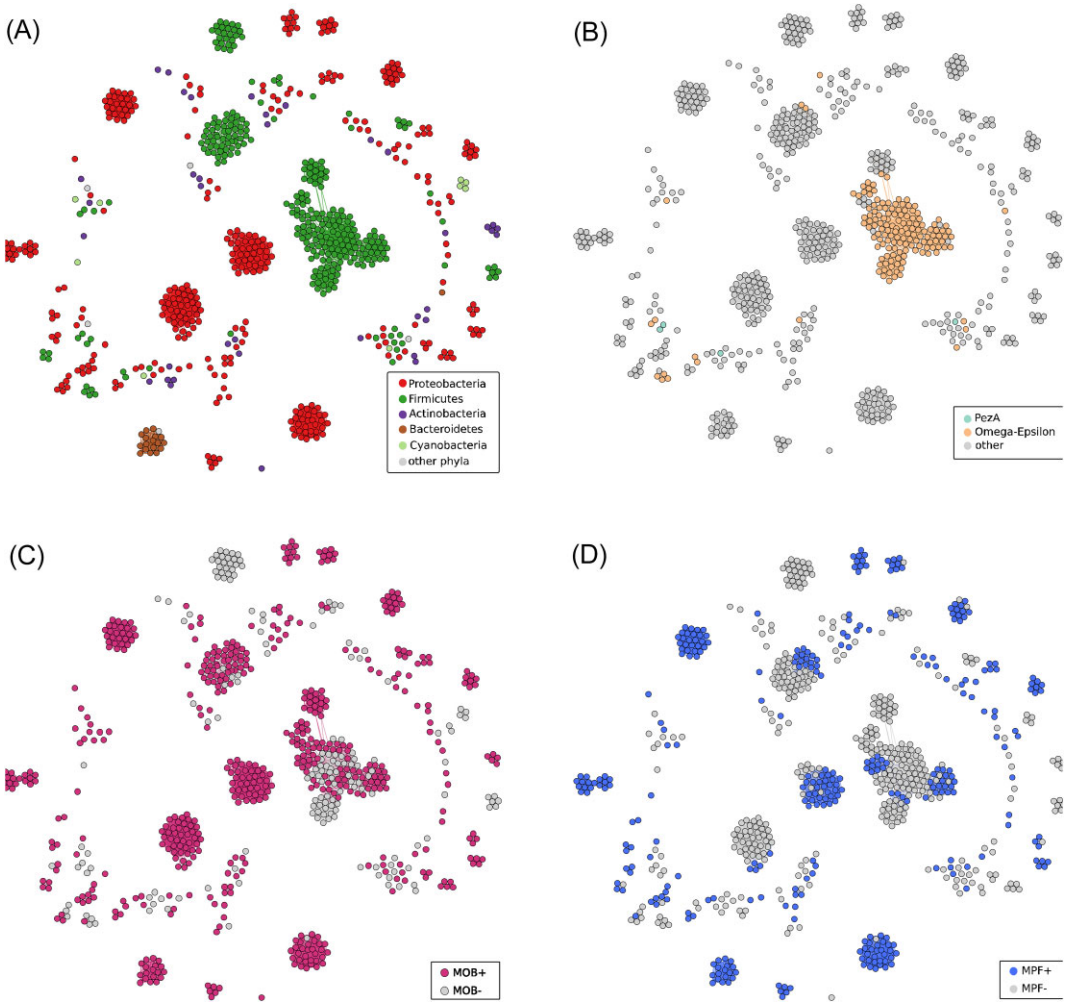

Figure 11. ANI similarity network of plasmids encoding *pezT/zeta* genes. For a dataset of 706 *pezT/zeta*-encoding plasmids (nodes), ANI_{L50} scores of all pairwise comparisons were calculated as described by Redondo-Salvo et al. (2020). When different from 0 they are represented as edges connecting the members of the corresponding plasmid pair. The ForceAtlas2 algorithm implemented in Gephi (Bastian et al. 2009) was applied to obtain the network layout. The network was coloured by (A) phylum of the plasmid host (Table S4, Supporting Information), (B) cognate antitoxin (Table S1, Supporting Information), (C) relaxase MOB class assigned by MOBscan (Garcillán-Barcia et al. 2020) (Table S4, Supporting Information), and (D) MPF type assigned by CONJscan (Cury et al. 2020) (Table S4, Supporting Information).

failure, successful occasions may occur, like those examples in which *S. pneumoniae* planktonic cells migrate from their habitual nasopharynx niche to colonize the lungs (Baquero 2009, Gamez and Hammerschmidt 2012). Later on, pneumococcal cells can migrate to the blood or the cerebrospinal fluid, where huge transcriptome changes have been observed (Pettersen et al. 2022). Cell responses to these fluctuations may vary between shrinking their cytoplasmic content (Shi et al. 2021), entering into a dormancy state (Dubnau and Losick 2006), or by stochastic separation from a formerly genetically identical population into two or more distinct subpopulations, i.e. a bi- or multistable response, respectively (Jayaraman 2008, Armbruster et al. 2019). The bistable response has been reported for situations in which changes in a part of the population would occur (Rao et al. 2002, Dubnau and Losick 2006 , Veening et al. 2008). In this situation, the nichome transcriptional regulatory proteins would trigger sets of genes that will benefit the entire population as a whole, even though one or more of the subpopulations may lose viability or be eliminated.

Among the nichome-encoded proteins, TAs could constitute a set of defence resources that would play an important role during colonization. However, like many other defence systems, TAs seem to have evolved under a strong selective pressure exerted by the fluctuating environments in which bacteria live. Such pressure would lead to a forced evolution that could be uncoupled from the evolution of the rest of the respective genomes. In the case of Type II TAs, we could envisage that the community changes that take place in stressful conditions would reduce the bacterial growth rate. This, in turn, could lead to the triggering of protease synthesis, antitoxin degradation, and toxin-mediated growth rate decline, if not cell death. This view, however, has been denied based on two solid arguments: (i) lack of experimental results that show antitoxin cleavage by proteases during stressful conditions, and (ii) antitoxins might be partially unfolded (and thus prone to degradation) before binding to their cognate toxins, but once the complex is formed the antitoxins would be properly folded, and thus not a substrate for proteases anymore (Song and Wood 2020a). If this were the case, the activation of toxins could be the result of insufficient antitoxin synthesis. We may argue, however, that the involvement of TAs as a response to stress might not be general for all bacteria or TAs. Nevertheless, it is also true that a majority of the experiments on TA activation have been performed in the heterologous host *E. coli* and not in the original

host, which may not be the ideal experimental approach to draw general conclusions.

In the case of the two pneumococcal higher eukaryotes and prokaryotes nucleotide-binding (HEPN) RNases (Pillon et al. 2021) studied by our group (RelBE and YefM–YoeB), we have shown their involvement in processes related to colonization, like biofilm formation and oxidative stress when expressed in the cognate host (Chan et al. 2018). Such participation was not observed when the TA tested was PezAT (Chan and Espinosa 2016a).

PezT/Zeta toxins target the biosynthesis of the bacterial cell wall and are most likely evolutionary unrelated to the HEPN RNase toxins. Conservation was always found at the level of the toxin counterpart, whereas variations have been observed in the antitoxins, perhaps the most intriguing example being the $PezAT^{Mtb}$ antitoxin because it has an RHH conformation rather than the HTH one found in the *S. pneumoniae* counterpart, making it a most unusual PezA antitoxin (Tandon et al. 2019). Examples of solo toxin genes have been found in other systems than PezAT (Makarova et al. 2009, Chan et al. 2012, Jurėnas et al. 2022; this work). When we searched for PezT toxin in all bacteria, many PezT-like proteins not associated with PezA or Epsilon antitoxins were found, perhaps because they may not have been annotated, reported or studied as active TAs. These findings show that the identification and characterization of 'just one more' TA pair may overlook novel features that might not be evident by a single inspection of the DNA sequence of the loci. Thus, further studies on these PezT/Zeta-like homologues are clearly needed as current literature on these family of toxins showed that we have barely scratched the tip of the iceberg and many more interesting variants of these toxins and their antitoxin counterparts await future discoveries.

Type II TAs were supposed to be constructed as relatively simple operons composed of two genes and their protein products autoregulate their synthesis. However, some Type II TAs exhibit more complex organizations, as exemplified by the tripartite operon omega–epsilon–zeta (Ceglowski et al. 1993) or the Type IIb of *M. tuberculosis*, in which an (as)RNA participates in the regulation of the toxin synthesis (Dawson et al. 2022). Other complex situations have also been found. First, the PacTA of *P. aeruginosa* plays a role as a classical Type II TA and also regulates iron homeostasis (Song et al. 2022). Second, the Doc toxin is homologous to the core of the Type III Secretion System (T3SS) effector AvrB of *P. syringae* (Kinch et al. 2009), whereas AvrRxo1, another TSS3 effector from *Xanthomonas oryzae* pv. *oryzicola* seems to be homologous to the PezT toxin (Triplett et al. 2016). And third, an intriguing relationship between the T4SS Vbh (carried by plasmid pVbh of *B. schoenbuchensis*) and the VirB T4SS showed that Vbh is a canonical conjugation system. In addition to it, this conjugative secretion system is also used to export the FicTA-related TA (VbhTA) as an interbacterial effector protein complex (Harms et al. 2017). These evolutionary links between TAs and bacterial secretion systems throw a most interesting light on the complexity of these apparently simple bacterial modules.

More recent searches have shown that toxins exhibiting RNase activity may belong to different evolutionary families than the rest of Type II TAs because they can be considered ancestors of the HEPN RNases (Makarova et al. 2020, Pillon et al. 2021). RNase-toxins seem to be ancestors of the CRISPR–Cas family VI, thus creating a novel scenario in which TAs could be a set of bacterial mechanisms developed by bacteria to defend from MGEs invasion and that may have usurped functions related to other bacterial effectors (Harms et al. 2017, Makarova et al. 2020). All these findings have opened new avenues to our, at present, still limited view of bacterial TAs, leading to the conclusion that fresh approaches and different classifications of TA modules, perhaps based on the activity of the toxin rather than from their organization should be considered.

Authors' contributions

The outline of the review and its first draft was conceived by WTC and ME and was later corrected by CCY. MPGB performed all the bioinformatics analyses. All subsequent versions of the manuscript were successively corrected by all authors until a final text was approved.

Acknowledgements

Thanks are due to friends and colleagues for never-ending scientific discussions. Apologies are also due to those colleagues that think they are under cited. We are thankful to Monica Fontenla for the improvements in the quality of the artwork and to Milagros Rodríguez Bueno for help with obtaining a waiver from CSIC. We also acknowledge the support of the publication fee by the CSIC Open Access Publication Support Initiative through its Unit of Information Resources for Research (URICI), especially to Inmaculada Ramos Hita.

Supplementary data

Supplementary data is available at *FEMSRE Journal* online.

Conflict of interest: The authors declare no conflict of interest.

Funding

This research did not receive specific external funding. However, the laboratories of MPGB and of ME were supported by the Spanish Ministry of Science and Innovation, grants MCIN/AEI/10.13039/501100011033 PID2020-117923GB-I00, and PID2019-104553RB-C21, respectively. CCY was supported by the Malaysian Ministry of Higher Education grant FRGS/1/2019/SKK11/UNISZA/02/1.

References

Akarsu H, Bordes PM, Bigot M *et al.* TASmania: a bacterial Toxin-Antitoxin Systems database. *PLOS Comp Biol* 2019;**15**:e1006946.

Aprianto R, Slager J, Holsappel S *et al.* High-resolution analysis of the pneumococcal transcriptome under a wide range of infection-relevant conditions. *Nucleic Acids Res* 2018;**46**:9990–10006.

Arbing MA, Handelman SK, Kuzin AP *et al.* Crystal structures of Phd-Doc, HigA, and YeeU establish multiple evolutionary links between microbial growth-regulating toxin-antitoxin systems. *Structure* 2010;**18**:996–1010.

Armbruster CR, Lee CK, Parker-Gilham J *et al.* Heterogeneity in surface sensing suggests a division of labor in *Pseudomonas aeruginosa* populations. *Elife* 2019;**8**:e45084.

Bai X-H, Chen H-J, Jiang Y-L *et al.* Structure of pneumococcal peptidoglycan hydrolase LytB reveals insights into the bacterial cell wall remodeling and pathogenesis. *J Biol Chem* 2014;**289**:23403–16.

Baquero F. Environmental stress and evolvability in microbial systems. *Clin Microbiol Infect* 2009;**15**:5–10.

Bastian M, Heymann S, Jacomy M. Gephi: an open source software for exploring and manipulating networks. In: *Proceedings of the International AAAI Conference on Weblogs and Social Media*. Palo Alto, CA:

AAAI Press, 2009. https://gephi.org/users/publications/. (1 June 2023, date last accessed).

Behnke D, Golubkov VI, Malke H *et al.* Restriction endonuclease analysis of group A streptococcal plasmids determining resistance to macrolides, lincosamides and streptogramin-B antibiotics. *FEMS Microbiol Lett* 1979;**6**:5–9.

Bernard P, Couturier M. Cell killing by the F plasmid CcdB protein involves poisoning of DNA-topoisomerase II complexes. *J Mol Biol* 1992;**226**:735–45.

Bertram R, Schuster CF. Post-transcriptional regulation of gene expression in bacterial pathogens by toxin-antitoxin systems. *Front Cell Infect Microbiol* 2014;**4**:6.

Blanchet C, Pasi M, Zakrzewska K *et al.* CURVES+ web server for analyzing and visualizing the helical, backbone and groove parameters of nucleic acid structures. *Nucleic Acids Res* 2011;**39**: W68–73.

Bonabal S, Darfeuille F. Preventing toxicity in toxin-antitoxin systems: an overview of regulatory mechanisms. *Biochimie* 2023. https://doi.org/10.1016/j.biochi.2023.07.013.

Bordes P, Genevaux P. Control of toxin-antitoxin Systems by proteases in *Mycobacterium tuberculosis*. *Front Mol Biosci* 2021;**8**:691399.

Boss L, Kędzierska B. Bacterial toxin-antitoxin systems' cross-interactions-implications for practical use in medicine and biotechnology. *Toxins* 2023;**15**:380.

Bravo A, Ortega S, de Torrontegui G *et al.* Killing of *Escherichia coli* cells modulated by components of the stability system ParD of plasmid R1. *Mol Gen Genet* 1988;**215**:146–51.

Bravo A, Ruiz-Cruz S, Alkorta I *et al.* When humans met superbugs: strategies to tackle bacterial resistances to antibiotics. *Biomol Concepts* 2018;**9**:216–26.

Brown BL. Lord DM Grigoriu S Peti W Page R The *Escherichia coli* toxin MqsR destabilizes the transcriptional repression complex formed between the antitoxin MqsA and the *mqsRA* operon promoter.. *J Biol Chem* 2013;**288**:1286–94.

Brown JS, Gilliland SM, Spratt BG *et al.* A locus contained within a variable region of pneumococcal pathogenicity island 1 contributes to virulence in mice. *Infect Immun* 2004;**72**:1587–93.

Brzozowska I, Zielenkiewicz U. Regulation of toxin–antitoxin systems by proteolysis. *Plasmid* 2013;**70**:33–41.

Brzozowska I, Zielenkiewicz U. The ClpXP protease is responsible for the degradation of the Epsilon antidote to the Zeta toxin of the streptococcal pSM19035 plasmid. *J Biol Chem* 2014;**289**: 7514–23.

Camacho AG, Misselwitz R, Behlke J *et al.* *In vitro* and *in vivo* stability of the *epsilon2zeta2* protein complex of the broad host-range *Streptococcus pyogenes* pSM19035 addiction system. *Biol Chem* 2002;**383**:1701–13.

Capella-Gutiérrez S, Silla-Martínez JM, Gabaldón T. trimAl: a tool for automated alignment trimming in large-scale phylogenetic analyses. *Bioinformatics* 2009;**25**:1972–3.

Castro-Roa D, Garcia-Pino A, De Gieter S *et al.* The Fic protein Doc uses an inverted substrate to phosphorylate and inactivate EF-tu. *Nat Chem Biol* 2013;**9**:811–7.

Ceglowski P, Boitsov A, Chai S *et al.* Analysis of the stabilization system of pSM19035-derived plasmid pBT233 in *Bacillus subtilis*. *Gene* 1993;**136**:1–12.

Chan W-T, Domenech M, Moreno-Córdoba I *et al.* The *Streptococcus pneumoniae yefM-yoeB* and *relBE* toxin-antitoxin operons participate in oxidative stress and biofilm formation. *Toxins* 2018; **10**:378.

Chan W-T, Yeo CC, Sadowy E *et al.* Functional validation of putative toxin-antitoxin genes from the Gram-positive pathogen *Streptococcus pneumoniae*: *p hd-doc* is the fourth bona-fide operon. *Front Microbiol* 2014;**5**:677.

Chan WT, Balsa D, Espinosa M. One cannot rule them all: are bacterial toxins-antitoxins druggable?. *FEMS Microbiol Rev* 2015;**39**:522–40.

Chan WT, Espinosa M, Yeo CC. Keeping the wolves at bay: antitoxins of prokaryotic type II toxin-antitoxin systems. *Front Mol Biosci* 2016;**3**:9.

Chan WT, Espinosa M. The antibacterials that have yet to be found. Atlas of Science. 2016a. https://atlasofscience.org/the-antibacterials-that-have-yet-to-be-found/. (1 June 2023, date last accessed).

Chan WT, Espinosa M. The *Streptococcus pneumoniae pezAT* toxin-antitoxin system reduces β-lactam resistance and genetic competence. *Front Microbiol* 2016b;**7**:1322.

Chan WT, Moreno-Córdoba I, Yeo CC *et al.* Toxin-antitoxin genes of the gram-positive pathogen *Streptococcus pneumoniae*: so few and yet so many. *Microbiol Mol Biol Rev* 2012;**76**:773–91.

Chan WT, Moreno-Córdoba I, Yeo CC *et al.* *Toxin-Antitoxin Loci in Streptococcus pneumoniae*. *Prokaryotic Toxin-Antitoxins*, Gerdes K (ed.), Berlin, Heidelberg: Springer, 2013, 315–39.

Chan WT, Nieto C, Harikrishna JA *et al.* Genetic regulation of the *yefM-yoeB* $_{Spn}$ toxin-antitoxin locus of *Streptococcus pneumoniae*. *J Bacteriol* 2011;**193**:4612–25.

Cherny I, Rockah L, Gazit E. The YoeB toxin is a folded protein that forms a physical complex with the unfolded YefM antitoxin. *J Biol Chem* 2005;**280**:30063–72.

Colombini L, Cuppone AM, Tirziu M *et al.* The mobilome-enriched genome of the competence-deficient *Streptococcus pneumoniae* BM6001, the original host of Integrative Conjugative Element Tn5253, is phylogenetically distinct from historical pneumococcal genomes. *Microorganisms* 2023;**11**:1646.

Croucher NJ, Vernikos GS, Parkhill J *et al.* Identification, variation and transcription of pneumococcal repeat sequences. *BMC Genomics* 2011;**12**:120.

Cruz JW, Rothenbacher FP, Maehigashi T *et al.* Doc toxin is a kinase that inactivates elongation factor Tu. *J Biol Chem* 2014;**289**:7788–98.

Cury J, Abby SS, Doppelt-Azeroual O *et al.* Identifying conjugative plasmids and integrative conjugative elements with CONJscan. In: *Horizontal Gene Transfer: Methods and Protocols*. de la Cruz F (ed.), New York: Springer, 2020, 265–83.

Dawson CC, Cummings JE, Starkey JM *et al.* Discovery of a novel type IIb RelBE toxin-antitoxin system in *Mycobacterium tuberculosis* defined by co-regulation with an antisense RNA. *Mol Microbiol* 2022;**117**:1419–33.

De Bruyn P, Girardin Y, Loris R. Prokaryote toxin–antitoxin modules: complex regulation of an unclear function. *Protein Sci* 2021;**30**:1103–13.

de la Hoz AB, Ayora S, Sitkiewicz I *et al.* Plasmid copy-number control and better-than-random segregation genes of pSM19035 share a common regulator. *Proc Natl Acad Sci USA* 2000;**97**:728–33.

de la Hoz AB, Pratto F, Misselwitz R *et al.* Recognition of DNA by Omega protein from the broad-host range *Streptococcus pyogenes* plasmid pSM19035: analysis of binding to operator DNA with one to four heptad repeats. *Nucleic Acids Res* 2004;**32**:3136–47.

Díaz-Orejas R, Espinosa M, Yeo CC. The importance of the expendable: toxin–antitoxin genes in plasmids and chromosomes. *Front Microbiol* 2017;**8**:1479.

Domenech M, Garcia E. The N-acetylglucosaminidase LytB of *Streptococcus pneumoniae* is involved in the structure and formation of biofilms. *Appl Environ Microbiol* 2020;**86**:e00280–00220.

Dubnau D, Losick R. Bistability in bacteria. *Mol Microbiol* 2006;**61**:564–72.

Eddy SR. A new generation of homology search tools based on probabilistic inference. *Genome Inform* 2009;**23**:205–11.

Edgar RC. MUSCLE: multiple sequence alignment with high accuracy and high throughput. *Nucleic Acid Res* 2004;**32**:1792–7.

Ferruz N, Schmidt S, Höcker B. ProtGPT2 is a deep unsupervised language model for protein design. *Nat Comm* 2022;**13**:4348.

Fraikin N, Goormaghtigh F, Van Melderen L. Type II toxin-antitoxin systems: evolution and revolutions. *J Bacteriol* 2020;**202**:e00763–00719.

Gamez G, Hammerschmidt S. Combat pneumococcal infections: adhesins as candidates for protein-based vaccine development. *Curr Drug Targets* 2012;**13**:323–37.

Ganaie F, Saad JS, McGee L *et al.* A new pneumococcal capsule type, 10D, is the 100th serotype and has a large *cps fragment* from an oral Streptococcus. *Mbio* 2020;**11**. https://doi.org/10.1128/mbio.00937-00920.

García E. Two putative glutamate decarboxylases of *Streptococcus pneumoniae* as possible antigens for the production of anti-GAD65 antibodies leading to type 1 diabetes mellitus. *Intl Microbiol* 2023;**26**:675–90.

García P, González MP, García E *et al.* LytB, a novel pneumococcal murein hydrolase essential for cell separation. *Mol Microbiol* 1999;**31**:1275–7.

Garcillán-Barcia MP, Pluta R, Lorenzo-Díaz F *et al.* The facts and family secrets of plasmids that replicate via the rolling-circle mechanism. *Microbiol Mol Biol Rev* 2022;**86**:e00222–00220.

Garcillán-Barcia MP, Redondo-Salvo S, Vielva L *et al.* MOBscan: automated annotation of MOB relaxases. In: *Horizontal Gene Transfer: Methods and Protocols*. de la Cruz F (ed.), New York: Springer, 2020, 295–308.

Geller BL, Marshall-Batty K, Schnell FJ *et al.* Gene-silencing antisense oligomers inhibit *Acinetobacter* growth *in vitro* and *in vivo*. *J Infect Dis* 2013;**208**:1553–60.

Gerdes K, Christensen KS, Lobner-Olensen A. Prokaryotic toxin-antitoxin stress response loci. *Nat Rev Microbiol* 2005;**3**:371–82.

Gerdes K, Maisonneuve E. Bacterial persistence and toxin-antitoxin loci. *Annu Rev Microbiol* 2012;**66**:103–23.

Gerdes K, Rasmussen PB, Molin S. Unique type of plasmid maintenance function: postsegregational killing of plasmid-free cells. *Proc Natl Acad Sci U S A* 1986;**83**:3116–20.

Germain E, Castro-Roa D, Zenkin N, *et al.* Molecular mechanism of bacterial persistence by HipA. *Mol Cell* 2013;**52**:248–54.

Glanville DG, Gazioglu O, Marra M *et al.* Pneumococcal capsule expression is controlled through a conserved, distal cis-regulatory element during infection. *PLOS Path* 2023;**19**:e1011035.

Hanage WP, Fraser C, Tang J *et al.* Hyper-recombination, diversity, and antibiotic resistance in pneumococcus. *Science* 2009;**324**:1454–7.

Harms A, Brodersen DE, Mitarai N *et al.* Toxins, targets, and triggers: an overview of toxin-antitoxin biology. *Mol Cell* 2018;**70**:768–84.

Harms A, Liesch M, Körner J *et al.* A bacterial toxin-antitoxin module is the origin of inter-bacterial and inter-kingdom effectors of *Bartonella*. *PLOS Genet* 2017;**13**:e1007077.

Harms A, Stanger FV, Dehio C. Biological diversity and molecular plasticity of FIC domain proteins. *Annu Rev Microbiol* 2016;**70**:341–60.

Harms A, Stanger FV, Scheu PD *et al.* Adenylylation of gyrase and topo IV by FicT toxins disrupts bacterial DNA topology. *Cell Rep* 2015;**12**:1497–507.

Harvey RM, Stroeher UH, Ogunniyi AD *et al.* A variable region within the genome of *Streptococcus pneumoniae* contributes to strain-strain variation in virulence. *PLoS ONE* 2011;**6**:e19650.

Haudiquet M, de Sousa JM, Touchon M *et al.* Selfish, promiscuous and sometimes useful: how mobile genetic elements drive horizontal gene transfer in microbial populations. *Phil Trans R Soc B Biol Sci* 2022;**377**:20210234.

Hernández-Arriaga AM, Chan WT, Espinosa M *et al.* Conditional activation of toxin-antitoxin systems: postsegregational killing and beyond. *Microbiol Spectr* 2014;**2**:26104348.

Hernández-Arriaga AM, Rubio-Lepe TS, Espinosa M *et al.* Repressor CopG prevents access of RNA polymerase to promoter and actively dissociates open complexes. *Nucl Acids Res* 2009;**37**:4799–811.

Hoang DT, Chernomor O, von Haeseler A *et al.* UFBoot2: improving the ultrafast bootstrap approximation. *Mol Biol Evol* 2017;**35**:518–22.

Hobson C, Chan AN, Wright GD. The antibiotic resistome: a guide for the discovery of natural products as antimicrobial agents. *Chem Rev* 2021;**121**:3464–94.

Ikuta KS, Swetschinski LR, Robles Aguilar G *et al.* Global mortality associated with 33 bacterial pathogens in 2019: a systematic analysis for the Global Burden of Disease Study 2019. *Lancet North Am Ed* 2022;**400**:2221–48.

Inniss NL, Prehna G, Morrison DA. The pneumococcal σ^X activator, ComW, is a DNA-binding protein critical for natural transformation. *J Biol Chem* 2019;**294**:11101–18.

Inouye M. The discovery of mRNA interferases: implication in bacterial physiology and application to biotechnology. *J Cell Physiol* 2006;**209**:670–6.

Jaffe A, Ogura T, Hiraga S. Effects of the *ccd* function of the F plasmid on bacterial growth. *J Bacteriol* 1985;**163**:841–9.

Jayaraman R. Bacterial persistence: some new insights into an old phenomenon. *J Biosc* 2008;**33**:795–805.

Jurėnas D, Fraikin N, Goormaghtigh F *et al.* Biology and evolution of bacterial toxin–antitoxin systems. *Nat Rev Microbiol* 2022;**20**:335–50.

Jurėnas D, Van Melderen L. The variety in the common theme of translation inhibition by type II toxin–antitoxin systems. *Front Genet* 2020;**11**:262.

Kalyaanamoorthy S, Minh BQ, Wong TKF *et al.* ModelFinder: fast model selection for accurate phylogenetic estimates. *Nat Meth* 2017;**14**:587–9.

Kamruzzaman M, Wu AY, Iredell JR. Biological functions of type II toxin-antitoxin systems in bacteria. *Microorganisms* 2021;**9**:1276.

Kang S-M, Kim D-H, Jin C *et al.* A systematic overview of type II and III toxin-antitoxin systems with a focus on druggability. *Toxins* 2018;**10**:515.

Kaspy I, Rotem E, Weiss N, *et al.* HipA-mediated antibiotic persistence via phosphorylation of the glutamyl-tRNA-synthetase. *Nat Commun* 2013;**4**:3001.

Kędzierska B, Hayes F. Emerging roles of toxin-antitoxin modules in bacterial pathogenesis. *Molecules* 2016b;**21**:790.

Kędzierska B, Hayes F. Transcriptional control of toxin–antitoxin expression: keeping toxins under wraps until the time is right. In: *Stress and Environmental Regulation of Gene Expression and Adaptation in Bacteria*, Hoboken: John Wiley & Sons, Inc, 2016a, 463–72.

Kędzierska B, Potrykus K, Szalewska-Pałasz A *et al.* Insights into transcriptional repression of the homologous toxin-antitoxin cassettes *yefM-yoeB* and *axe-txe*. *Int J Mol Sci* 2020;**21**:9062.

Khoo SK, Loll B, Chan WT *et al.* Molecular and structural characterization of the PezAT chromosomal toxin-antitoxin system of the human pathogen *Streptococcus pneumoniae*. *J Biol Chem* 2007;**282**:19606–18.

Kim D-H, Kang S-M, Park SJ *et al.* Functional insights into the *Streptococcus pneumoniae* HicBA toxin–antitoxin system based on a structural study. *Nucleic Acids Res* 2018;**46**:6371–86.

Kim SY, Eun H-J, Lee J *et al.* Structural-guided fragment-based drug discovery applied to antitoxin, MAB3862 opens a new possibility of exploring the toxin and antitoxin for antibiotics. *bioRxiv* 2022. https://doi.org/10.1101/2022.05.14.491971.

Kinch LN, Yarbrough ML, Orth K *et al.* Fido, a novel AMPylation domain common to Fic, Doc, and AvrB. *PLoS ONE* 2009;**4**:e5818.

Knutsen E, Johnsborg O, Quentin Y *et al.* BOX elements modulate gene expression in *Streptococcus pneumoniae*: impact on the fine-tuning of competence development. *J Bacteriol* 2006;**188**:8307–12.

Labbé CM, Laconde G, Kuenemann MA *et al.* iPPI-DB: a manually curated and interactive database of small non-peptide inhibitors of protein–protein interactions. *Drug Discov Today* 2013;**18**:958–68.

Lee K-Y, Lee B-J. Structure, biology, and therapeutic application of toxin-antitoxin systems in pathogenic bacteria. *Toxins* 2016;**8**:305.

Lehnherr H, Maguin E, Jafri S *et al.* Plasmid addiction genes of bacteriophage P1: *d oc*, which causes cell death on curing of prophage, and *phd*, which prevents host death when prophage is retained. *J Mol Biol* 1993;**233**:414–28.

Leplae R, Geeraerts D, Hallez R *et al.* Diversity of bacterial type II toxin–antitoxin systems: a comprehensive search and functional analysis of novel families. *Nucleic Acids Res* 2011;**39**:5513–25.

LeRoux M, Laub MT. Toxin-antitoxin systems as phage defense elements. *Annu Rev Microbiol* 2022;**76**:21–43.

Letunic I, Bork P. Interactive Tree of Life (iTOL) v4: recent updates and new developments. *Nucleic Acids Res* 2019;**47**:W256–9.

Lewis AM, Willard DJH, Manesh MJ *et al.* Stay or go: sulfolobales biofilm dispersal is dependent on a bifunctional VapB antitoxin. *Mbio* 2023;**0**:e00053–00023.

Li M, Guo N, Song G *et al.* Type II toxin- antitoxin systems in *Pseudomonas aeruginosa*. *Toxins* 2023;**15**:164.

Lioy VS, Machon C, Tabone M *et al.* The ζ toxin induces a set of protective responses and dormancy. *PLoS ONE* 2012;**7**:e30282.

Lioy VS, Rey O, Balsa D *et al.* A toxin-antitoxin module as a target for antimicrobial development. *Plasmid* 2010;**63**:31–39.

Liu G, Catacutan DB, Rathod K *et al.* Deep learning-guided discovery of an antibiotic targeting *Acinetobacter baumannii*. *Nat Chem Biol* 2023; 37231267. https://doi.org/10.1038/s41589-023-01349-8.

Liu M, Li X, Xie Y *et al.* ICEberg 2.0: an updated database of bacterial integrative and conjugative elements. *Nucleic Acids Res* 2019;**47**:D660–5.

Lobato-Márquez D, Díaz-Orejas R, García-del Portillo F. Toxin-antitoxins and bacterial virulence. *FEMS Microbiol Rev* 2016;**40**:592–609.

Loris R, Garcia-Pino A. Disorder- and dynamics-based regulatory mechanisms in toxin–antitoxin modules. *Chem Rev* 2014;**114**:6933–47.

Loris R, Marianovsky I, Lah J *et al.* Crystal structure of the intrinsically flexible addiction antidote MazE. *J Biol Chem* 2003;**278**:28252–7.

Mahmoudi M, Sadeghifard N, Maleki A *et al. relBE* toxin-antitoxin system as a reliable anti-biofilm target in *Pseudomonas aeruginosa*. *J Appl Microbiol* 2022;**133**:683–95.

Makarova K, Wolf YI, Koonin EV. Comprehensive comparative-genomic analysis of type 2 toxin-antitoxin systems and related mobile stress response systems in prokaryotes. *Biol Direct* 2009;**4**:19.

Makarova KS, Wolf YI, Iranzo J *et al.* Evolutionary classification of CRISPR–Cas systems: a burst of class 2 and derived variants. *Nat Rev Microbiol* 2020;**18**:67–83.

Margolis E, Levin BR. The evolution of bacteria-host interactions: virulence and the immune over-response. In: *Evolutionary Biology of Bacterial and Fungal Pathogens*, Baquero F, Nombela C, Cassell GH, Gutierrez-Fuentes JA (eds), Washington: ASM Press, 2007, 3–12.

Martin B, Humbert O, Camara M *et al.* A highly conserved repeated DNA element located in the chromosome of *Streptococcus pneumoniae*. *Nucleic Acids Res* 1992;**20**:3479–83.

Meinhart A, Alings C, Strater N *et al.* Crystallization and preliminary X-ray diffraction studies of the epsilon-zeta addiction system encoded by *Streptococcus pyogenes* plasmid pSM19035. *Acta Crystallogr D Biol Crystallogr* 2001;**57**:745–7.

Meinhart A, Alonso JC, Strater N *et al.* Crystal structure of the plasmid maintenance system *epsilon/zeta*: functional mechanism of toxin zeta and inactivation by *epsilon2zeta2* complex formation. *Proc Natl Acad Sci USA* 2003;**100**:1661–6.

Meyers J, Fabian B, Brown N. *De novo* molecular design and generative models. *Drug Discov Today* 2021;**26**:2707–15.

Michael CA, Gillings MR, Blaskovich MAT *et al.* The antimicrobial resistance crisis: an inadvertent, unfortunate but nevertheless informative experiment in evolutionary biology. *Front Ecol Evol* 2021;**9**. https://doi.org/10.3389/fevo.2021.692674.

Mistry J, Chuguransky S, Williams L *et al.* Pfam: the protein families database in 2021. *Nucleic Acids Res* 2020;**49**:D412–9.

Moreno-Córdoba I, Chan W-T, Nieto C *et al.* Interactions of the *Streptococcus pneumoniae* toxin-antitoxin RelBE proteins with their target DNA. *Microorganisms* 2021;**9**:851.

Moreno-Córdoba I, Diago-Navarro E, Barendregt A *et al.* The toxin-antitoxin proteins RelBE2*Spn* of *Streptococcus pneumoniae*: characterization and association to their DNA target. *Proteins* 2012;**80**:1834–46.

Moreno-del Álamo M, Marchisone C, Alonso JC. Antitoxin ε reverses toxin ζ-facilitated ampicillin dormants. *Toxins* 2020;**12**:801.

Moreno-del Álamo M, Tabone M, Muñoz-Martínez J *et al.* Toxin ζ reduces the ATP and modulates the uridine diphosphate-N-AcetylGlucosamine Pool. *Toxins* 2019;**11**:29.

Moscoso M, García E. Transcriptional regulation of the capsular polysaccharide biosynthesis locus of *Streptococcus pneumoniae*: a bioinformatic analysis. *DNA Res* 2009;**16**:177–86.

Moscoso M. García E López R Biofilm formation by *Streptococcus pneumoniae*: role of choline, extracellular DNA, and capsular polysaccharide in microbial accretion.. *J Bacteriol* 2006;**188**:7785–95.

Mulchandani R, Wang Y, Gilbert M *et al.* Global trends in antimicrobial use in food-producing animals: 2020 to 2030. *PLOS Glob Pub Health* 2023;**3**:e0001305.

Murayama K, de la Hoz AB, Alings C *et al.* Crystallization and preliminary X-ray diffraction studies of *Streptococcus pyogenes* plasmid pSM19035-encoded omega transcriptional repressor. *Acta Crystallogr D Biol Crystallogr* 1999;**55**:2041–2.

Murayama K, Orth P, de la Hoz AB *et al.* Crystal structure of Omega transcriptional repressor encoded by *Streptococcus pyogenes* plasmid pSM19035 at 1.5 A resolution. *J Mol Biol* 2001;**314**:789–96.

Murray CJL, Ikuta KS, Sharara F *et al.* Global burden of bacterial antimicrobial resistance in 2019: a systematic analysis. *Lancet North Am Ed* 2022;**399**:629–55.

Mutschler H, Gebhardt M, Shoeman RL *et al.* A novel mechanism of programmed cell death in bacteria by toxin-antitoxin systems corrupts peptidoglycan synthesis. *PLoS Biol* 2011;**9**:e1001033.

Mutschler H, Meinhart A. Type II toxin-antitoxin loci: the Epsilon/Zeta family. In: *Prokaryotic Toxin-Antitoxins*. Gerdes K (ed.), Berlin, Heidelberg: Springer, 2013, 205–23.

Mutschler H, Meinhart A. ε/ζ systems: their role in resistance, virulence, and their potential for antibiotic development. *J Mol Med* 2011;**89**:1183–94.

Mutschler H, Reinstein J, Meinhart A. Assembly dynamics and stability of the pneumococcal Epsilon Zeta antitoxin toxin (PezAT) system from *Streptococcus pneumoniae*. *J Biol Chem* 2010;**285**:21797–806.

Nadeem SF, Gohar UF, Tahir SF *et al.* Antimicrobial resistance: more than 70 years of war between humans and bacteria. *Crit Rev Microbiol* 2020;**46**:578–99.

Nguyen L-T, Schmidt HA, von Haeseler A *et al.* IQ-TREE: a fast and effective stochastic algorithm for estimating maximum-likelihood phylogenies. *Mol Biol Evol* 2014;**32**:268–74.

Nieto C, Cherny I, Khoo SK *et al.* The *yefM-yoeB* toxin-antitoxin systems of *Escherichia coli* and *Streptococcus pneumoniae*: functional and structural correlation. *J Bacteriol* 2007;**189**:1266–78.

Nieto C, Pellicer T, Balsa D *et al.* The chromosomal *relBE2* toxin-antitoxin locus of *Streptococcus pneumoniae*: characterization and use of a bioluminescence resonance energy transfer assay to detect toxin-antitoxin interaction. *Mol Microbiol* 2006;**59**:1280–96.

Nieto C, Sadowy E, de la Campa AG *et al.* The *relBE2Spn* toxin-antitoxin system of *Streptococcus pneumoniae*: role in antibiotic tolerance and functional conservation in clinical isolates. *PLoS ONE* 2010;**5**:e11289.

O'Brien KL, Wolfson LJ, Watt JP *et al.* Burden of disease caused by *Streptococcus pneumoniae* in children younger than 5 years: global estimates. *Lancet North Am Ed* 2009;**374**:893–902.

Oggioni MR, Claverys JP. Repeated extragenic sequences in prokaryotic genomes: a proposal for the origin and dynamics of the RUP element in *Streptococcus pneumoniae*. *Microbiology* 1999;**145**:2647–53.

Ogura T, Hiraga S. Mini-F plasmid genes that couple host cell division to plasmid proliferation. *Proc Natl Acad Sci USA* 1983;**80**:4784–8.

Pabo CO, Sauer RT. Protein-DNA recognition. *Annu Rev Biochem* 1984;**53**:293–321.

Page R, Peti W. Toxin-antitoxin systems in bacterial growth arrest and persistence. *Nat Chem Biol* 2016;**12**:208–14.

Park S, Son W, Lee B. Structural overview of toxin-antitoxin systems in infectious bacteria: a target for developing antimicrobial agents. *Biochim Biophys Acta* 2013;**1834**:1155–67.

Paul P, Sahu BR, Suar M. Plausible role of bacterial toxin–antitoxin system in persister cell formation and elimination. *Mol Oral Microbiol* 2019;**34**:97–107.

Pecota DC. Wood TK Exclusion of T4 phage by the *hok/sok* killer locus from plasmid R1. *J Bacteriol* 1996;**178**:2044–50.

Pedersen K, Zavialov AV, Pavlov MY *et al.* The bacterial toxin RelE displays codon-specific cleavage of mRNAs in the ribosomal A site. *Cell* 2003;**112**:131–40.

Peplow M. Skeleton crew. *Nature* 2023;**618**:21–24.

Pettersen JS, Høg F, Fabricius N *et al.* Global transcriptional responses of pneumococcus to human blood components and cerebrospinal fluid. *Front Microbiol* 2022;**13**:1060583.

Pillon MC, Gordon J, Frazier MN *et al.* HEPN RNases - an emerging class of functionally distinct RNA processing and degradation enzymes. *Crit Rev Biochem Mol Biol* 2021;**56**:88–108.

Qiu J, Zhai Y, Wei M *et al.* Toxin–antitoxin systems: classification, biological roles, and applications. *Microbiol Res* 2022;**264**:127159.

Rao CV, Wolf DM, Arkin AP. Control, exploitation and tolerance of intracellular noise. *Nature* 2002;**420**:231–7.

Redondo-Salvo S, Bartomeus-Peñalver R, Vielva L *et al.* COPLA, a taxonomic classifier of plasmids. *BMC Bioinf* 2021;**22**:390.

Redondo-Salvo S, Fernández-López R, Ruiz R *et al.* Pathways for horizontal gene transfer in bacteria revealed by a global map of their plasmids. *Nat Comm* 2020;**11**:3602.

Rocker A, Meinhart A. A cis-acting antitoxin domain within the chromosomal toxin-antitoxin module EzeT of *Escherichia coli* quenches toxin activity. *Mol Microbiol* 2015;**97**:589–604.

Rocker A, Peschke M, Kittilä T *et al.* The ng_ζ1 toxin of the gonococcal epsilon/zeta toxin/antitoxin system drains precursors for cell wall synthesis. *Nat Comm* 2018;**9**:1686.

Rosendahl S, Tamman H, Brauer A *et al.* Chromosomal toxin-antitoxin systems in *Pseudomonas putida* are rather selfish than beneficial. *Sci Rep* 2020;**10**:9230.

Równicki M, Lasek ç, Trylska J *et al.* Targeting type II toxin-antitoxin systems as antibacterial strategies. *Toxins* 2020;**12**:568.

Santoro F, Iannelli F, Pozzi G. Genomics and genetics of *Streptococcus pneumoniae*. *Microbiol Spectrum* 2019;**7**. https://doi.org/10.1128/microbiolspec.GPP3-0025-2018.

Schleif R, Espinosa M. Where to from here?. *Front Mol Biosci* 2022;**9**:848444.

Schumacher MA, Piro KM, Xu W *et al.* Molecular mechanisms of HipA-mediated multidrug tolerance and its neutralization by HipB. *Science* 2009;**323**:396–401.

Schwarz FV, Perreten V, Teuber M. Sequence of the 50-kb conjugative multiresistance plasmid pRE25 from *Enterococcus faecalis* RE25. *Plasmid* 2001;**46**:170–87.

Semanjski M, Germain E, Bratl K, *et al.* The kinases HipA and HipA7 phosphorylate different substrate pools in Escherichia coli to promote multidrug tolerance. *Sci Signal* 2018;**11**.

Senior AW, Evans R, Jumper J *et al.* Improved protein structure prediction using potentials from deep learning. *Nature* 2020;**577**:706–10.

Shi H, Westfall CS, Kao J *et al.* Starvation induces shrinkage of the bacterial cytoplasm. *Proc Natl Acad Sci USA* 2021;**118**:e2104686118.

Shi X-X, Wang Z-Z, Wang F *et al.* ACFIS 2.0: an improved web-server for fragment-based drug discovery via a dynamic screening strategy. *Nucleic Acids Res* 2023;**51**:W25–32.

Singh G, Yadav M, Ghosh C *et al.* Bacterial toxin-antitoxin modules: classification, functions, and association with persistence. *Curr Res Microb Sci* 2021;**2**:100047.

Slager J, Aprianto R, Veening J-W. Refining the pneumococcal competence regulon by RNA sequencing. *J Bacteriol* 2019;**201**:e00780–00718.

Sletvold H, Johnsen PJ, Hamre I *et al.* Complete sequence of *Enterococcus faecium* pVEF3 and the detection of an *ω-ε-ζ* toxin-antitoxin module and an ABC transporter. *Plasmid* 2008;**60**:75–85.

Solano-Collado V, Ruiz-Cruz S, Lorenzo-Díaz F *et al.* Recognition of streptococcal promoters by the pneumococcal SigA protein. *Front Mol Biosci* 2021;**8**:666504.

Song S, Wood TK. A primary physiological role of toxin/antitoxin systems is phage inhibition. *Front Microbiol* 2020b;**11**:1895.

Song S, Wood TK. Post-segregational killing and phage inhibition are not mediated by cell death through toxin/antitoxin systems. *Front Microbiol* 2018;**9**:814.

Song S, Wood TK. Toxin/antitoxin system paradigms: toxins bound to antitoxins are not likely activated by preferential antitoxin degradation. *Adv Biosys* 2020a;**4**:1900290.

Song Y, Zhang S, Ye Z *et al.* The novel type II toxin–antitoxin PacTA modulates *Pseudomonas aeruginosa* iron homeostasis by obstructing the DNA-binding activity of Fur. *Nucleic Acids Res* 2022;**50**:10586–600.

Sonika S, Singh S, Mishra S *et al.* Toxin-antitoxin systems in bacterial pathogenesis. *Heliyon* 2023;**9**:e14220.

Steinegger M, Söding J. MMseqs2 enables sensitive protein sequence searching for the analysis of massive data sets. *Nat Biotech* 2017;**35**:1026–8.

Sterckx YG, Garcia-Pino A, Haesaerts S *et al.* The ParE2-PaaA2 toxin-antitoxin complex from *Escherichia coli* O157 forms a heterodode-

camer in solution and in the crystal. *Acta Crystallogr Sect F Struct Biol Cryst Commun* 2012;**68**:724–9.
Sterckx YGJ, Jové T, Shkumatov AV *et al.* A unique hetero-hexadecameric architecture displayed by the *E. coli* O157 PaaA2-ParE2 antitoxin-toxin complex. *J Mol Biol* 2016;**482**:1589–603.
Suarez-Mendez CA, Sousa A, Heijnen JJ *et al.* Fast "feast/famine" cycles for studying microbial physiology under dynamic conditions: a case study with *saccharomyces cerevisiae*. *Metabolites* 2014;**4**:347–72.
Tafroji W, Margyaningsih NI, Khoeri MM *et al.* Antibacterial activity of medicinal plants in Indonesia on *Streptococcus pneumoniae*. *PLoS ONE* 2022;**17**:e0274174.
Tandon H, Sharma A, Sandhya S *et al. Mycobacterium tuberculosis* Rv0366c-Rv0367c encodes a non-canonical PezAT-like toxin-antitoxin pair. *Sci Rep* 2019;**9**:1163.
Tettelin H, Nelson KE, Paulsen IT *et al.* Complete genome sequence of a virulent isolate of *Streptococcus pneumoniae*. *Science* 2001;**293**:498–506.
Tong AB, Burch JD, McKay D *et al.* Could AlphaFold revolutionize chemical therapeutics?. *Nat Struct Mol Biol* 2021;**28**:771–2.
Triplett LR, Shidore T, Long J *et al.* AvrRxo1 Is a bifunctional type III secreted effector and toxin-antitoxin system component with homologs in diverse environmental contexts. *PLoS ONE* 2016;**11**:e0158856.
Troeger C, Blacker B, Khalil IA *et al.* Estimates of the global, regional, and national morbidity, mortality, and aetiologies of lower respiratory infections in 195 countries, 1990–2016: a systematic analysis for the Global Burden of Disease Study 2016. *The Lancet Infect Dis* 2018;**18**:1191–210.
Tsukuda M, Nakashima N, Miyazaki K. Counterselection method based on conditional silencing of antitoxin genes in *Escherichia coli*. *J Biosci Bioeng* 2015;**5**:591–5.
Van Melderen L, Dao Thi M-H, Lecchi P *et al.* ATP-dependent degradation of CcdA by Lon protease. Effects of secondary structure and heterologous subunit interactions. *J Biol Chem* 1996;**271**:27730–8.
Vang Nielsen S, Turnbull KJ, Roghanian M, *et al.* Serine-Threonine Kinases Encoded by Split hipA Homologs Inhibit Tryptophanyl-tRNA Synthetase. *mBio* 2019;**10**.
Varadi M, Anyango S, Deshpande M *et al.* AlphaFold Protein Structure Database: massively expanding the structural coverage of protein-sequence space with high-accuracy models. *Nucleic Acids Res* 2022;**50**:D439–44.
Veening J-W, Smits WK, Kuipers OP. Bistability, epigenetics, and bet-hedging in bacteria. *Annu Rev Microbiol* 2008;**62**:193–210.
Volante A, Carrasco B, Tabone M *et al.* The interaction of ω2 with the RNA polymerase β' subunit functions as an activation to repression switch. *Nucleic Acids Res* 2015;**43**:9249–61.
Weihofen WA, Cicek A, Pratto F *et al.* Structures of Omega repressors bound to direct and inverted DNA repeats explain modulation of transcription. *Nucleic Acid Res* 2006;**34**:1450–8.
Wen Y, Behiels E, Devreese B. Toxin-antitoxin systems: their role in persistence, biofilm formation and pathogenicity. *Pathog Dis* 2014a;**70**:240–9.
Wen Y, Behiels E, Felix J *et al.* The bacterial antitoxin HipB establishes a ternary complex with operator DNA and phosphorylated toxin HipA to regulate bacterial persistence. *Nucleic Acids Res* 2014b;**42**:10134–47.
Williams JJ, Hergenrother PJ. Artificial activation of toxin-antitoxin systems as an antibacterial strategy. *Trends Microbiol* 2012;**20**:291–8.
Winther KS, Brodersen DE, Brown AK *et al.* VapC20 of *Mycobacterium tuberculosis* cleaves the sarcin–Ricin loop of 23S rRNA. *Nat Comm* 2013;**4**:2796.
Woodgate J, Zenkin N. Transcription–translation coupling: recent advances and future perspectives. *Mol Microbiol* 2023. https://doi.org/10.1111/mmi.15076.
Wu H-J, Wang AHJ, Jennings MP. Discovery of virulence factors of pathogenic bacteria. *Curr Opin Chem Biol* 2008;**12**:93–101.
Xie Y, Wei Y, Shen Y *et al.* TADB 2.0: an updated database of bacterial type II toxin-antitoxin loci. *Nucleic Acids Res* 2018;**46**:D749–d753.
Xue L, Yue J, Ke J *et al.* Distinct oligomeric structures of the YoeB–YefM complex provide insights into the conditional cooperativity of type II toxin–antitoxin system. *Nucleic Acids Res* 2020;**48**:10527–41.
Yamaguchi Y, Inouye M. Regulation of growth and death in *Escherichia coli* by toxin–antitoxin systems. *Nat Rev Microbiol* 2011;**9**:779–90.
Yamaguchi Y, Inouye M. Type II toxin-antitoxin loci: the *mazEF* family. In: *Prokaryotic Toxin-Antitoxins*, Gerdes K (ed.), Berlin, Heidelberg: Springer, 2013, 107–36.
Yuan J, Sterckx Y, Mitchenall LA *et al. Vibrio cholerae* ParE2 poisons DNA gyrase via a mechanism distinct from other gyrase inhibitors. *J Biol Chem* 2010;**285**:40397–408.
Zhang S-P, Wang Q, Quan S-W *et al.* Type II toxin–antitoxin system in bacteria: activation, function, and mode of action. *Biophys Rep* 2020;**6**:68–79.
Zhang Y, Song X, Chen C *et al.* Structural insights of the toxin-antitoxin system VPA0770-VPA0769 in *Vibrio parahaemolyticus*. *Intl J Biol Macromol* 2023;**242**:124755.
Zhang Y, Zhang J, Hoeflich KP *et al.* MazF cleaves cellular mRNAs specifically at ACA to block protein synthesis in *Escherichia coli*. *Mol Cell* 2003;**12**:913–23.

Received 26 June 2023; **revised** 24 August 2023; **accepted** 7 September 2023